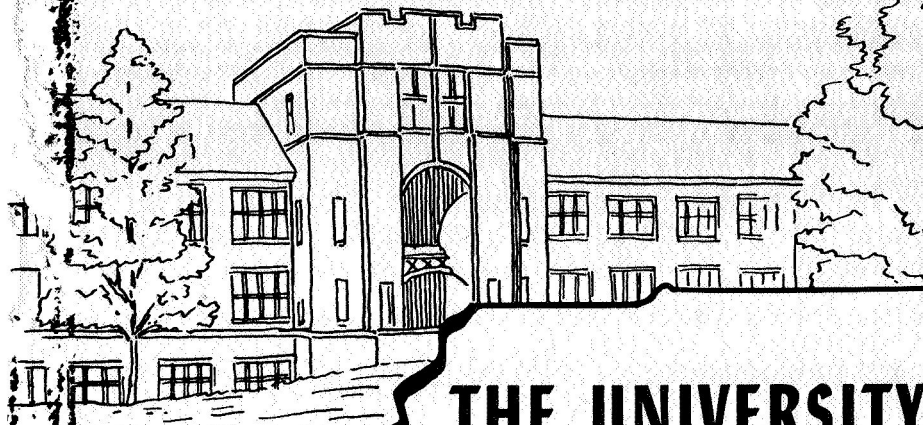


N 69 39 93 8

ME 69-T57-6

NASA CR 106264

**CASE FILE
COPY**



THE UNIVERSITY OF TENNESSEE

DEPARTMENT OF MECHANICAL
AND AEROSPACE ENGINEERING

AN INVESTIGATION OF INTERFACE STABILITY AND ITS
RELATION TO GAS INGESTION IN VISCOSEALS

by
Charles F. Fisher, Jr.

August 1969

Knoxville, Tennessee 37916

This document has been approved for public release
and sale; its distribution is unlimited.

ME 69-T57-6

The University of Tennessee
Department of Mechanical and Aerospace Engineering

AN INVESTIGATION OF INTERFACE STABILITY AND ITS RELATION
TO GAS INGESTION IN VISCOSEALS

by
Charles F. Fisher, Jr.

Supported by
NATIONAL AERONAUTICS AND SPACE ADMINISTRATION
DEPARTMENT OF DEFENSE

Prepared Under
NASA Grant NGR-43-001-003

This document has been approved for public release
and sale; its distribution is unlimited.

August 1969
Knoxville, Tennessee 37916

FOREWARD

This document is submitted as an interim report on the viscoseal investigation, which is part of the University of Tennessee Dynamic Sealing research program. Support for this work was provided by grant NGR-43-001-003 from the National Aeronautics and Space Administration and contract N00014-68-A-0144 with the Office of Naval Research.

This report was submitted to the University of Tennessee in partial fulfillment of the requirements for the degree of Doctor of Philosophy, with a major in Mechanical Engineering, and is presented here with minor changes in format.

The author wishes to express his appreciation to Professor W. K. Stair of the Department of Mechanical and Aerospace Engineering for his invaluable contribution in providing guidance and moral support throughout this investigation. Mr. R. L. Johnson and Mr. L. P. Ludwig, NASA Lewis Research Center, also provided helpful suggestions for which the author is personally grateful.

Approved: _____

W. K. Stair
W. K. Stair

C. F. Fisher, Jr.
C. F. Fisher, Jr.

ABSTRACT

A fundamental study of the stability of a dynamic gas-liquid interface between rotating cylinders is reported. The study was initiated for the purpose of seeking factors which have a significant role in the process of gas ingestion, or gas entrainment, in viscoseals.

The simplified model of smooth, cylindrical surfaces was selected for mathematical tractability and to provide a visual study, using a transparent acrylic housing, without the obscurity of the more complex fluid flow resulting from the presence of the grooved surfaces employed in viscoseals. The visual study was supplemented by employing stroboscopic photography and high-speed motion picture photography.

A phenomenological mechanism of gas ingestion was established, theoretically and experimentally. It was found that gas entrainment can result from a gas-liquid interface instability caused by a velocity of a portion of the interface toward the more viscous fluid and/or an acceleration of a portion of the interface toward the more dense fluid. Results of the study indicate that surface tension tends to stabilize the interface and prevent or delay gas ingestion.

It is concluded that gas ingestion in viscoseals is an essentially inherent phenomenon which cannot be readily eliminated through optimization of the viscoseal geometry.

A brief discussion is given on the implications of the interface stability study in the operation of journal bearings, face seals, and buffered bushing seals, in addition to a discussion of its application to viscoseals.

Eccentricity, shaft runout, and vibrations are credited with contributing to conditions necessary for the instability of an interface in rotating machinery.

TABLE OF CONTENTS

CHAPTER	PAGE
I. INTRODUCTION.	1
II. ANALYTICAL STUDY.	9
Mathematical Model.	9
Stability Analysis - Viscous Effects.	11
Stability Analysis - Acceleration Effects	30
III. EXPERIMENTAL STUDY.	39
Experimental Facility	39
Description of Experimental Investigation	43
IV. EXPERIMENTAL RESULTS.	47
V. DISCUSSION.	57
VI. CONCLUSIONS AND RECOMMENDATIONS	64
BIBLIOGRAPHY.	66
VITA.	69

LIST OF FIGURES

FIGURE	PAGE
1. Elements of a Typical Viscoseal.	2
2. Model for Analysis of Interface Separating Two Fluids Confined Between Parallel Plates Having Relative Motion Parallel to the Interface.	10
3. Model for Analysis of a Disturbed Interface Separating Two Viscous Fluids Moving Transverse to the Interface and Confined Between Parallel Plates Having Relative Motion Parallel to the Interface	16
4. Schematic Representation of Pressure Field in a Viscous Liquid Separated from a Gas by an Unstable Interface	21
5. Model for Analysis of a Disturbed Interface Separating Two Viscous Fluids Moving Transverse to the Interface and Confined Between Parallel Plates Having Relative Motion not Parallel to the Interface	26
6. Model for Analysis of the Stability of an Accelerated Interface Separating Two Fluids Having Different Densities.	31

LIST OF FIGURES, continued

FIGURE	PAGE
7. Interface Study Facility	40
8. Experimental Facilities.	42
9. Fingers of Air and 50% Mixture of Glycerine and Water at Shaft Speed of 50 rpm	49
10. Motion Picture Frame Sequence Showing Development of Fingers in 50% Glycerine- 50% Water Solution. Shaft Rotation of 26.5° Between Frames, Shaft Speed - 440 rpm, Clearance - 0.006 inch.	50
11. Retouched Motion Picture Frame Sequence Showing Development of Fingers in 50% Glycerine-50% Water Solution. Shaft Rotation of 26.5° Between Frames, Shaft Speed - 440 rpm, Clearance - 0.006 inches.	51
12. Air-Distilled Water Interface Region at Shaft Speed of 1100 rpm.	54

LIST OF SYMBOLS

SYMBOL	DESCRIPTION	UNIT
<u>English Alphabet</u>		
a	Acceleration	inch/sec ²
c	Radial clearance	inch
g	Gravitational acceleration	inch/sec ²
K	Wave number = $2\pi/L$	inch ⁻¹
L	Wavelength of interface disturbance	inch
L _u	Wavelength of unstable disturbance	inch
m	Time coefficient	sec ⁻¹
P	Pressure	lb _f /inch ²
Re	Reynolds number = $\rho Uc/\mu$	dimensionless
R ₁	Interface radius of curvature in a plane normal to flat plates	inch
R ₂	Interface radius of curvature in a plane parallel to flat plates	inch
S	Interface displacement from mean position of interface	inch
t	Time	sec
T	Surface tension	lb _f /inch
u	Velocity component in x-direction	inch/sec
\bar{u}	Mean velocity component in x-direction	inch/sec

SYMBOL	DESCRIPTION	UNIT
U	Surface velocity of shaft	inch/sec
v	Velocity component in y-direction	inch/sec
\bar{v}	Mean velocity component in y-direction	inch/sec
V	Plate velocity in y-direction	inch/sec
w	Velocity component in z-direction	inch/sec
x,y	Coordinates parallel to moving surface	inch
z	Coordinate normal to moving surface	inch

Greek Alphabet

ρ	Density	$\text{lb}_m/\text{inch}^3$
μ	Absolute viscosity	$\text{lb}_f \text{ sec}/\text{inch}^2$
ϕ	Velocity potential	inch^2/sec

Subscripts

1	denotes Fluid 1
2	denotes Fluid 2

CHAPTER I

INTRODUCTION

A fundamental study of the stability of a dynamic gas-liquid interface was initiated for the purpose of providing insight into the mechanism of gas ingestion in viscoseals.

A viscoseal is a dynamic shaft seal which develops a pressure gradient in the axial direction within the annular space between a shaft and housing having a relative angular velocity and normally not in contact with each other. Helical grooves are provided on the shaft and/or the housing, and the relative motion of the two surfaces causes a viscous pumping action on the fluid in the annular space, developing the desired pressure gradient in the axial direction and establishing a gas-liquid interface within the annulus. A typical viscoseal, with a grooved shaft and smooth housing, is shown in Figure 1.

Since the viscoseal does not depend on rubbing contact in providing sealing action, it offers the possibility of low wear rates and essentially zero-leakage rates for extended periods of operation. These considerations are important in space applications and nuclear operations, and also make the viscoseal an attractive contender for many

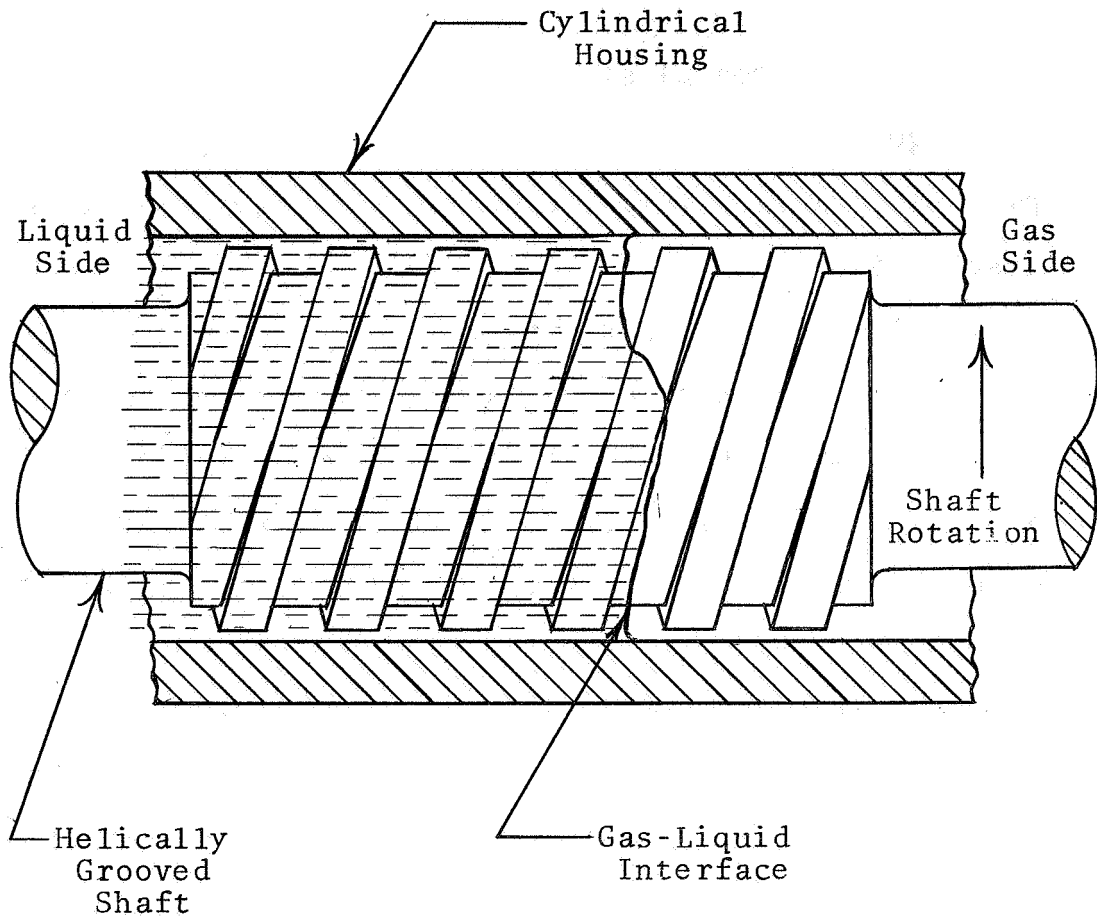


Figure 1. Elements of a typical viscoseal.

other industrial applications, particularly those involving high-speed rotating machinery.

The viscoseal is essentially the same physical apparatus as a screw extruder, a device of earlier origin operated for the primary purpose of producing a flow of a very viscous liquid or a plastic, usually under pressure. The first patent of an extruder employing a screw was taken out in 1879 by an Englishman named Gray [1]¹. John Royle developed a screw machine in the U.S. at the same time.

Lawaczeck [2] conducted tests with the viscopump in 1916 in an extension of the screw extruder concept to the performance of the viscoseal function of generating an axial pressure gradient while producing no net flow through the annulus.

An experimental screw oil pump, reported by Pearsall [3] in 1924, used a threaded shaft to produce a high-pressure oil flow, and also employed screw threads "to act as a gland and prevent the oil escaping" along a sleeve. Pearsall derived a relation between the volumetric flow rate and the outlet pressure. He commented that "when using such a thread to retain oil and prevent it leaking out the end of the bearing, it has been found in practice necessary to run

¹Numbers in brackets refer to similarly numbered references in the bibliography.

at a speed about two and a half times that given by the equations for no flow."

Rowell and Finlayson [4] presented an analysis of the screw viscosity pump in 1928 and commented on its "most immediately interesting application" in the field of bearing seals.

Interest in the viscoseal concept continued, but the subject received only a limited amount of attention until the needs for advanced sealing concepts in the space and nuclear programs gave impetus to the development of the viscoseal at a more rapid pace.

In 1963, McGrew and McHugh [5] reported an observed phenomenon which they called "seal breakdown" which appeared as a leakage of about one drop of liquid every three minutes and a decrease in the seal pressure. In their test rig arrangement, the axis of the shaft was parallel to the direction of the force of gravity. The liquid was above the interface and the leakage which was encountered was in the form of liquid dripping out the open end of the housing to the atmosphere. They studied the relation between the beginning of seal breakdown and the Reynolds number, Froude number, cavitation number, and Weber number. The Weber number, involving the fluid properties of density and surface tension, appeared to provide the best correlation with

seal breakdown, but was not conclusive. Three silicone fluids and water were tested. Seal breakdown for three of these fluids occurred in a range of Weber numbers from 800-1100. For the remaining fluid, which was one of the silicone fluids, the Weber number was 220 at the beginning of seal breakdown. Seal breakdown occurred under laminar flow conditions for another of the silicone fluids, while breakdown came in the transition range for one of the fluids and in the turbulent range for the other two fluids.

In a later experimental study, King [6] also employed a vertically mounted shaft with the liquid above the interface and observed a "secondary leakage brought on by splashing and instabilities at the liquid-vapor interface." Liquids tested by King were oil, water, and potassium. In the tests with water, the point at which the secondary leak could first be detected varied with the speed and radial clearance. At 0.0025 in. radial clearance, it was first noticed at 12,000 to 14,000 rpm; at 0.0029 in., it was noticed at 7,000 to 8,000 rpm; at 0.0044 in., it was noticed at the starting speed of 4,000 rpm. The Weber numbers corresponding to these points were 1290, 572, and 214, respectively. With a 0.0015 in. clearance, the shaft was operated at a speed up to 14,000 rpm with a corresponding Weber number of 883, but no leakage was noticed.

In experimental work reported by Stair [7] in 1965, the viscoseal shaft was oriented horizontally. During the course of this experimental work no evidence of a seal break was observed, but a phenomenon called air ingestion occurred. When the shaft speed was increased to a sufficiently high value, air bubbles were observed to rise in the transparent pressure tap lines, and bleeding the air from the lines would not stop the ingestion. The axial pressure gradient decreased and caused the air-water interface to move toward the atmospheric end of the seal, but there was no observed leakage except when the interface moved outside the annular space. At increased shaft speeds the amount of air ingestion would increase and in some cases the shaft reached a speed at which the pressure profile would become unstable and severe pressure pulsations were observed. Stair concluded from his data that air ingestion increases with shaft eccentricity and is reduced by using wider grooves. He noted [8] that no air ingestion was detectable with laminar operation of the seal.

An experimental study of gas ingestion was reported by Ludwig, Strom, and Allen [9] in March 1966. Test fluids used were water and sodium. In the tests with water, a transparent housing was used to permit visual observations of the gas ingestion region. For each fluid, tests were

made using a grooved shaft, and using a grooved housing, with the same groove depth, width, etc. used for each. Gas ingestion was found to be more pronounced with the grooved shaft, and the authors attributed the difference to the centrifuge action forcing bubbles into the grooves where they are pumped to the high-pressure end of the seal.

Although increasing attention has been given to the problem of gas ingestion, the basic mechanism causing it is not well understood. It is not understood how gas bubbles which become mixed with the liquid are transported to the high-pressure end of the seal. A separate question concerns the mechanism by which the interface becomes interrupted to permit the gas bubbles to become entrained in the liquid.

While the mechanism of seal breakdown or secondary leakage may be significantly different from that causing gas ingestion, both appear to result from some form of instability of the gas-liquid interface, suggesting the need for the study undertaken here.

A direct study of the stability of the dynamic interface actually encountered in the viscoseal presents an extremely difficult problem. Therefore, for the purpose of this investigation, a simplified model leading to a more basic study of the stability of a dynamic interface was

selected as a matter of practical expedience. The model which was chosen as having a significant similarity to the flow in a viscoseal, but sufficiently simple to permit an analytical study, was a gas and liquid confined in the annular space between the smooth surfaces of a stationary housing and a rotating cylinder. This model is the same as the viscoseal shown in Figure 1, page 2, except that a shaft with a smooth surface is substituted for the grooved shaft.

CHAPTER II

ANALYTICAL STUDY

I. MATHEMATICAL MODEL

The mathematical model for the analytical study was based on further simplifications of the flow model. Because of the small clearance between the surfaces having relative motion, the effects of curvature were considered to be of small magnitude in comparison with other variables of interest. Therefore, the model for mathematical analysis was obtained by assuming an interface between two incompressible, Newtonian fluids confined between two infinite flat plates moving at equal but oppositely directed velocities $U/2$ in the x -direction, as shown in Figure 2.

The theoretical analysis was approached by considering separately the effects of the fluid viscosities and the effects of fluid acceleration. The model for the analysis treating viscous effects was patterned after the work of Saffman and Taylor [10] in a study of the stability of an interface separating two viscous fluids confined between two closely spaced parallel plates with the fluids having a velocity perpendicular to the interface. The plates were assumed to be stationary and inertia effects were neglected

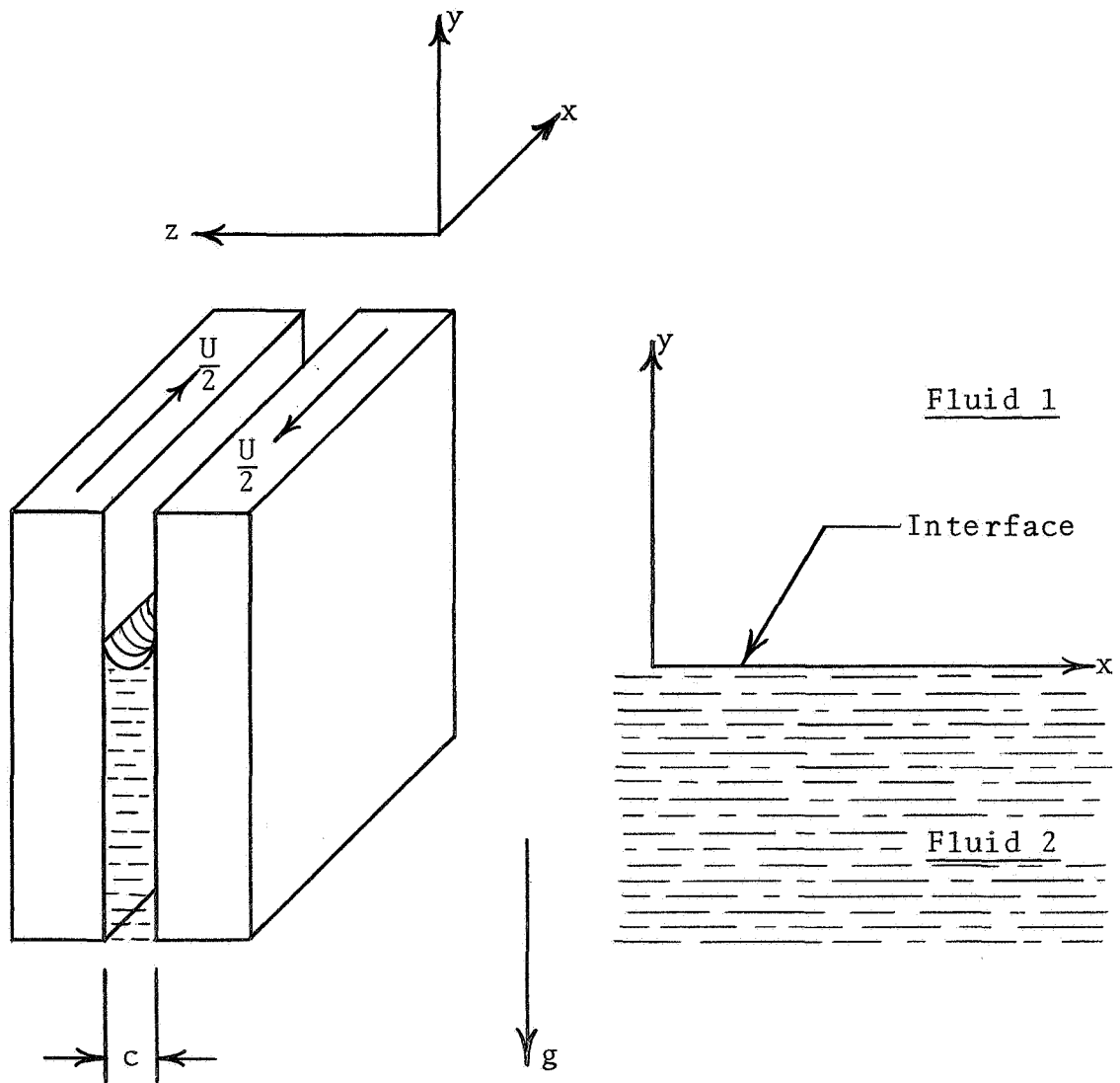


Figure 2. Model for analysis of interface separating two fluids confined between parallel plates having relative motion parallel to the interface.

in this analysis. The analysis taking acceleration effects into account was developed along lines similar to the work of Taylor [11] in a stability analysis of an interface separating two fluids of different densities when the fluids are accelerated in a direction normal to their mutual interface. His analysis was not restricted to a narrow space between two plates, and viscous effects were not included in the analysis.

II. STABILITY ANALYSIS - VISCOUS EFFECTS

For the Cartesian coordinate system shown in Figure 2, the Navier-Stokes equations are

$$\rho \frac{Du}{Dt} = - \frac{\partial P}{\partial x} + \mu \nabla^2 u; \quad (1)$$

$$\rho \frac{Dv}{Dt} = - \left(\frac{\partial P}{\partial y} + \rho g \right) + \mu \nabla^2 v; \quad (2)$$

$$\rho \frac{Dw}{Dt} = - \frac{\partial P}{\partial z} + \mu \nabla^2 w. \quad (3)$$

The clearance c between the plates is assumed to be small and the fluid motion is assumed to be everywhere parallel to the plates. Derivatives of velocity components in directions other than normal to the plates are assumed small in comparison with derivatives along the normal, and are neglected. If the acceleration terms are assumed to be

small, the equations of motion become

$$0 = - \frac{\partial P}{\partial x} + \mu \frac{\partial^2 u}{\partial z^2}, \quad (4)$$

and

$$0 = - \left(\frac{\partial P}{\partial y} + \rho g \right) + \frac{\partial^2 v}{\partial z^2}. \quad (5)$$

Integrating equations (4) and (5) with respect to z ,

$$\frac{\partial u}{\partial z} = \frac{1}{\mu} \frac{\partial P}{\partial x} z + C_1, \quad (6)$$

and

$$\frac{\partial v}{\partial z} = \frac{1}{\mu} \left(\frac{\partial P}{\partial y} + \rho g \right) z + C_2. \quad (7)$$

A second integration with respect to z yields

$$u = \frac{1}{2\mu} \frac{\partial P}{\partial x} z^2 + C_1 z + C_3, \quad (8)$$

and

$$v = \frac{1}{2\mu} \left(\frac{\partial P}{\partial y} + \rho g \right) z^2 + C_2 z + C_4. \quad (9)$$

The appropriate boundary conditions are,

$$\begin{aligned}
 \text{at } z = 0: \quad u &= -\frac{U}{2}; & v &= 0; \\
 \text{at } z = c: \quad u &= +\frac{U}{2}; & v &= 0.
 \end{aligned} \tag{10}$$

Substituting the boundary conditions into equations (8) and (9), the constants are

$$C_3 = -\frac{U}{2}, \tag{11}$$

$$C_4 = 0, \tag{12}$$

$$C_1 = \frac{U}{c} - \frac{1}{2\mu} \frac{\partial P}{\partial x} c, \tag{13}$$

$$C_2 = -\frac{1}{2\mu} \left(\frac{\partial P}{\partial y} + \rho g \right) c. \tag{14}$$

Equations (8) and (9) become

$$u = \frac{1}{2\mu} \frac{\partial P}{\partial x} z^2 + \frac{Uz}{c} - \frac{c}{2\mu} \frac{\partial P}{\partial x} z - \frac{U}{2}, \tag{15}$$

and

$$v = \frac{1}{2\mu} \left(\frac{\partial P}{\partial y} + \rho g \right) z^2 - \frac{c}{2\mu} \left(\frac{\partial P}{\partial y} + \rho g \right) z. \tag{16}$$

The mean velocities are

$$\bar{u} = \frac{1}{c} \int_0^c u \, dz, \tag{17}$$

$$\bar{v} = \frac{1}{c} \int_0^c v \, dz, \tag{18}$$

$$\bar{u} = \frac{1}{c} \left[\frac{1}{2\mu} \frac{\partial P}{\partial x} \frac{z^3}{3} + \frac{Uz^2}{2c} - \frac{c}{2\mu} \frac{\partial P}{\partial x} \frac{z^2}{2} - \frac{Uz}{2} \right]_0^c, \quad (19)$$

$$\bar{v} = \frac{1}{c} \left[\frac{1}{2\mu} \left(\frac{\partial P}{\partial y} + \rho g \right) \frac{z^3}{3} - \frac{c}{2\mu} \left(\frac{\partial P}{\partial y} + \rho g \right) \frac{z^2}{2} \right]_0^c, \quad (20)$$

$$\bar{u} = - \frac{c^2}{12\mu} \frac{\partial P}{\partial x}, \quad (21)$$

$$\bar{v} = - \frac{c^2}{12\mu} \left(\frac{\partial P}{\partial y} + \rho g \right). \quad (22)$$

The form of the equations for the mean velocities permits the introduction of a velocity potential ϕ , given by

$$\bar{u} = - \frac{c^2}{12\mu} \frac{\partial P}{\partial x} \equiv \frac{\partial \phi}{\partial x}, \quad (23)$$

and

$$\bar{v} = - \frac{c^2}{12\mu} \left(\frac{\partial P}{\partial y} + \rho g \right) \equiv \frac{\partial \phi}{\partial y}. \quad (24)$$

The interface is assumed to have a slight wave-like disturbance of wavelength

$$L = 2\pi/K, \quad (25)$$

described by

$$S = Be^{mt} \cos Kx, \quad (26)$$

which is the equation for the surface of separation of the

two fluids, and which gives the displacement of the interface from the mean position of the interface, as shown in Figure 3.

The stability problem becomes one of determining the algebraic sign of \underline{m} in equation (26). If \underline{m} is positive, the magnitude of the interface disturbance grows exponentially with time and the interface is unstable. Neutral stability exists when \underline{m} is zero, and the interface is stable to a small disturbance if the sign of \underline{m} is negative.

On the interface, the y-components of the velocities of the two fluids are equal, and are given by

$$\frac{\partial \phi_1}{\partial y} = \frac{\partial \phi_2}{\partial y} = \bar{v} + \frac{\partial S}{\partial t} \quad (27)$$

$$= \bar{v} + mBe^{mt} \cos Kx. \quad (28)$$

The solution of the continuity equation,

$$\nabla^2 \phi = 0, \quad (29)$$

must satisfy equation (28), and the disturbance velocity must vanish at infinity. The appropriate solutions are

$$\phi_1 = \bar{v}y - \frac{mB}{K} e^{mt} - Ky \cos Kx, \quad (30)$$

and

$$\phi_2 = \bar{v}y + \frac{mB}{K} e^{mt} + Ky \cos Kx. \quad (31)$$

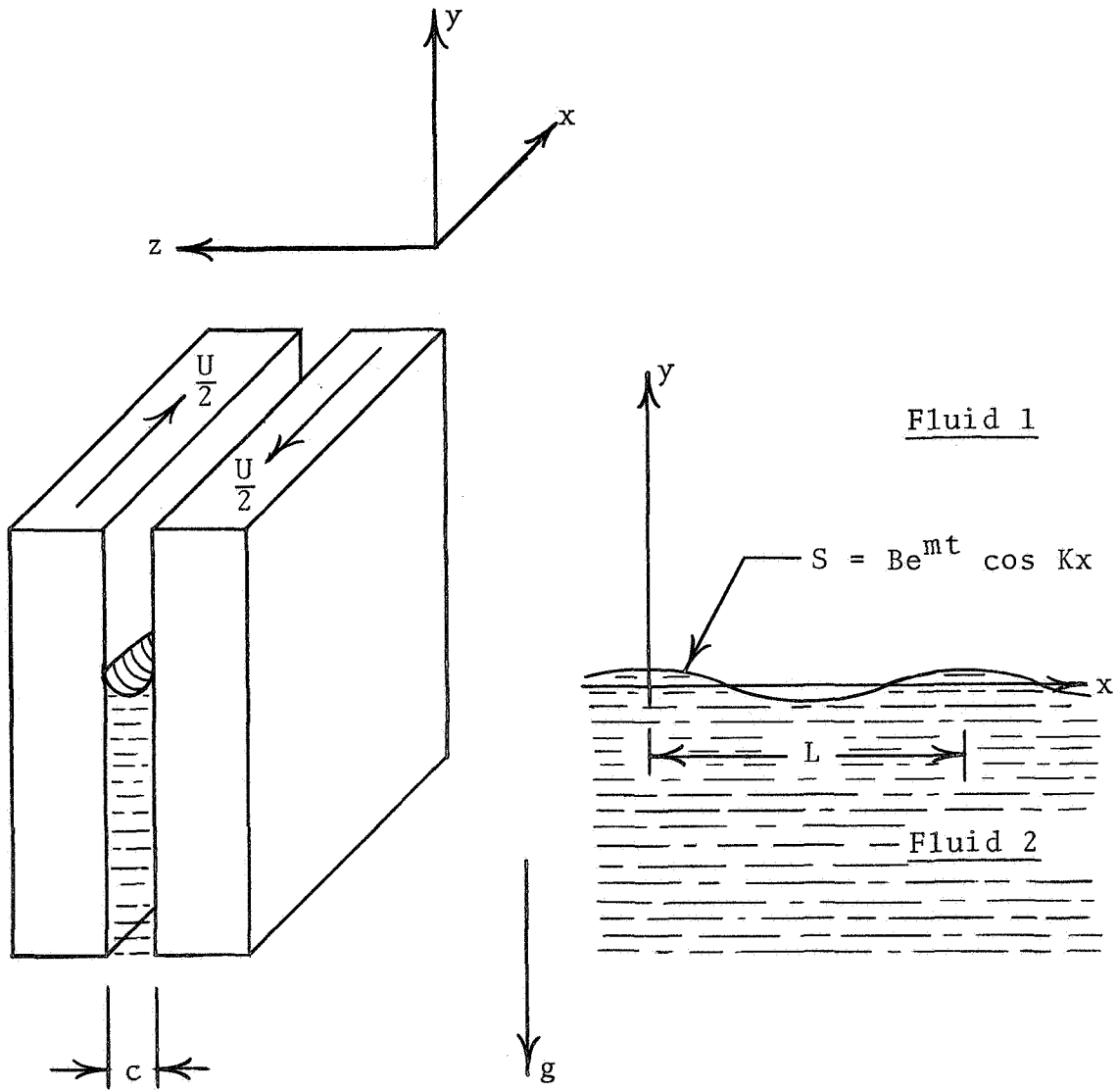


Figure 3. Model for analysis of a disturbed interface separating two viscous fluids moving transverse to the interface and confined between parallel plates having relative motion parallel to the interface.

Integrating equation (24) with respect to y , and substituting the velocity potentials from equations (30) and (31), the solutions for the pressures are

$$P_1 = - \frac{12\mu_1}{c^2} (\bar{v}y - \frac{mB}{K} e^{mt} - Ky \cos Kx) - \rho_1 gy + C_5, \quad (32)$$

and

$$P_2 = - \frac{12\mu_2}{c^2} (\bar{v}y + \frac{mB}{K} e^{mt} + Ky \cos Kx) - \rho_2 gy + C_6. \quad (33)$$

The difference between the pressures on the two sides of the interface will depend on the curvature of the interface [12], and may be expressed by the Laplace equation,

$$(P_1 - P_2) = T \left(\frac{1}{R_1} + \frac{1}{R_2} \right), \quad (34)$$

where T is the surface tension and R_1 and R_2 are the radii of curvature of the interface in mutually perpendicular planes. The interface curvature may depend in a rather complicated manner on such factors as the distance separating the plates, surface roughness, the materials of the solid surfaces, the liquid, and interface dynamics. For example, the contact angle for a receding interface would be expected to be less than the angle of contact of an advancing interface [13]. However, it is assumed here for

simplicity that the angles of contact with the solid surfaces are zero and that the radius R_1 is half the distance separating the solid surfaces, or

$$\frac{1}{R_1} = \frac{1}{c/2} \quad (35)$$

Because the interface disturbance was assumed to be small, the curvature in a plane parallel to the plates may be approximated by

$$\frac{1}{R_2} = \frac{\partial^2 S}{\partial x^2}, \quad (36)$$

When equations (35) and (36) are substituted into equation (34), the pressure difference becomes

$$(P_1 - P_2) = T \left(\frac{2}{c} + \frac{\partial^2 S}{\partial x^2} \right). \quad (37)$$

Substituting equation (26) into equation (37) and setting equation (37) equal to the pressure difference across the interface from equations (32) and (33) gives

$$\begin{aligned} T \left(\frac{2}{c} - BK^2 e^{mt} \cos Kx \right) &= - \frac{12\bar{v}S}{c^2} (\mu_1 - \mu_2) \\ &+ \frac{12mB}{c^2 K} (\mu_1 e^{mt} - KS + \mu_2 e^{mt} + KS) \cos Kx \\ &- (\rho_1 - \rho_2)gS + (C_5 - C_6). \end{aligned} \quad (38)$$

When S , as defined by equation (26), is zero, equation (38) reduces to

$$T\left(\frac{2}{c}\right) = (C_5 - C_6). \quad (39)$$

Substituting this into equation (38), then dividing through by S and multiplying through by $K = 2\pi/L$ gives

$$\frac{12\bar{m}}{c^2}(\mu_1 e^{-KS} + \mu_2 e^{+KS}) = \frac{2\pi}{L} \left[\frac{12\bar{v}}{c^2}(\mu_1 - \mu_2) + (\rho_1 - \rho_2)g \right] - \frac{8\pi^3 T}{L^3}. \quad (40)$$

A disturbance is unstable when the right-hand side of equation (40) is positive, since the left-hand side is positive when \bar{m} is positive. Therefore, the first term on the right-hand side of the equation must be positive and numerically larger than the second term on the right in order for a disturbance to be unstable.

Thus, surface tension tends to cause the interface to be stable to a small disturbance, and an interface velocity toward the more viscous fluid contributes toward the development of an instability.

Information concerning the wavelength L_u of unstable disturbances can also be obtained from equation (40). Setting the right-hand side of equation (40) to be greater

than zero,

$$L_u^2 \left[\frac{12\bar{v}}{c^2} (\mu_1 - \mu_2) + (\rho_1 - \rho_2)g \right] - 4\pi^2 T > 0, \quad (41)$$

which is the case for unstable disturbances, and solving for L_u gives

$$L_u > \frac{2\pi c T^{1/2}}{\left[12\bar{v}(\mu_1 - \mu_2) + c^2(\rho_1 - \rho_2)g \right]^{1/2}}. \quad (42)$$

When the necessary conditions exist, as given by equation (40), for small disturbances to be unstable, the wavelength of such unstable disturbances must be greater than the critical value given by equation (42). This value is proportional to the square root of the surface tension, so for the hypothetical case in which the surface tension is zero, the wavelength of unstable disturbances would not be limited to a minimum value. The result is the same as that found by Saffman and Taylor [10], even though the plates were considered to be stationary in their analysis.

That an unstable disturbance will continue to grow when it reaches a finite magnitude can be shown readily by a qualitative determination of the relative magnitude of pressure gradients at specific locations in Figure 4, where constant pressure lines in the liquid are sketched, but not

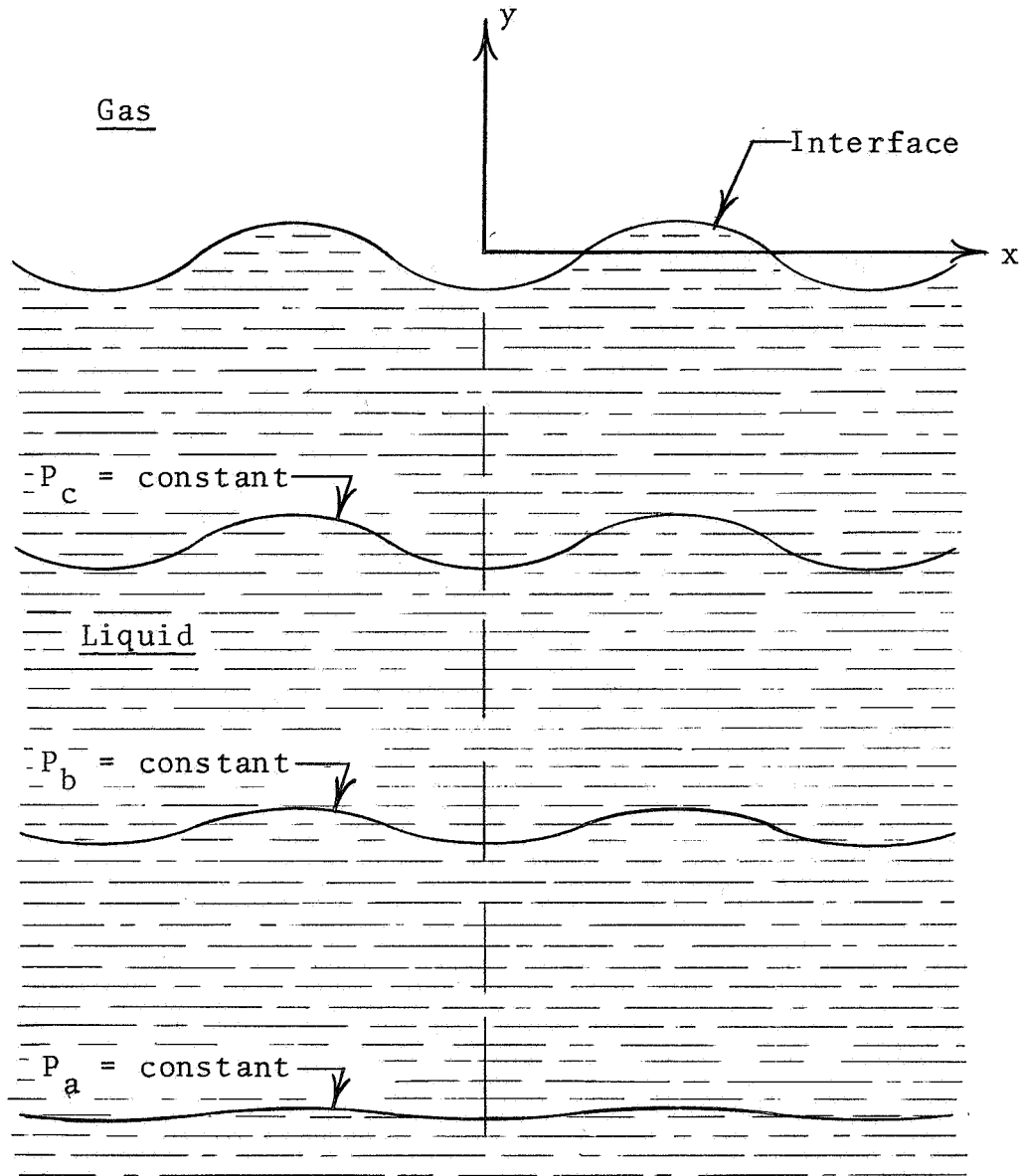


Figure 4. Schematic representation of pressure field in a viscous liquid separated from a gas by an unstable interface.

necessarily to scale. For the purpose of the qualitative analysis under consideration, assume that the gravitational force is normal to the plane of the plates in Figure 4. Since the primary concern here is with a gas-liquid interface, and liquid viscosities are usually much larger than the viscosity of gases, the viscosity of the gas may be ignored. Then with no pressure gradient required for the gas region, the pressure throughout the gas region has a uniform value. If the amplitude of the disturbance is small compared to its wavelength L , the pressure difference across the interface may be taken as approximately constant. Then the liquid pressure along the interface may be assumed to be approximately constant.

The pressure gradient in the liquid approaches a constant value at some distance from the interface. However, at a distance up to a few wavelengths away from the interface, the pressure gradient is a function of x , and along a line $y = \text{constant}$ has a larger magnitude in a region of nearest approach to the interface. Since the liquid velocity depends on the pressure gradient, the velocity of the liquid near the interface is greater in the region where the interface is leading than where it is lagging. Therefore, the portion of liquid which is lagging will continue to lag even further. Thus, the amplitude of the wave will continue to grow. Continued growth will

result in long "fingers" of gas extending into the liquid.

In the annular space between rotating cylinders, with an interface having a constant average position, the interface usually will oscillate axially about the mean position with a period equal to the time for one revolution of the rotating cylinder. This oscillation results from two unavoidable factors - eccentricity of mounting, and runout. Ignoring gravitational effects, the interface would be unstable only when moving toward the liquid. With the interface velocity in the opposite direction, the finite wave height, or finger length, would decrease. Therefore, fingers would be expected to form and grow to some finite length in a portion of the annulus, and then to become shorter and possibly disappear altogether in another portion of the annulus.

The fingers thus formed would attain a maximum length which depends on the overall displacement of the oscillating interface.

All of the fingers formed, as described above, would be expected to travel around the annulus at essentially half the surface speed of the rotating cylinder, although slight differences in their velocities could arise because of increasing or decreasing clearances along the path of fluid elements contained within such fingers, or variations in surface roughness, or other variations. Such velocity

differences could present an opportunity for a volume of air to become trapped within the liquid. If the top part of a liquid finger should travel with a tangential velocity slightly greater than that of the finger immediately preceding it, and for a sufficient length of time, the gap could be closed near the top and thus trap a volume of gas beneath the interface.

The chances of two adjacent fingers of liquid coming into contact with each other in this manner and trapping a volume of gas in the liquid would be enhanced by a high finger length-to-width ratio, i.e., by the presence of long, narrow fingers. Thus shorter wavelengths would be more conducive to trapping gas bubbles. Likewise, for a given wavelength, the greater the magnitude of the interface oscillation and thus the length to which a finger could grow, the greater the chance of entrainment of gas bubbles.

The mathematical model shown in Figure 2, page 10, was established for an interface parallel to the x-axis. When the interface in this theoretical model has a velocity, the liquid is either advancing on both surfaces, or receding on both surfaces. However, if the physical model - a rotating cylinder inside a housing - has eccentricity but no runout, the interface at a particular angular position on the stationary surface would have a constant axial location. But the axial location would vary with angular

position on the stationary cylinder and therefore the interface would be oscillating axially relative to the rotating cylinder. The reverse would be true for runout of the rotating cylinder but concentricity of mounting. Therefore, it remains to be determined what conditions would produce an instability when an interface is advancing or receding at different rates over the two surfaces between which the fluids are confined.

A slight modification of the mathematical model shown in Figure 2, page 10, can be made to approximate the desired conditions. The plates in Figure 2 are shown to have equal but oppositely directed velocities $U/2$ in the x -direction. One plate is further assigned a velocity V in the y -direction, as shown in Figure 5.

With this added condition imposed, appropriate boundary conditions are,

$$\begin{aligned} \text{at } z = 0: \quad u &= -\frac{U}{2}; \quad v = 0; \\ \text{at } z = c: \quad u &= +\frac{U}{2}; \quad v = V. \end{aligned} \tag{43}$$

The constants in equations (8) and (9) are unchanged, with the exception of C_2 , which becomes

$$C_2' = \frac{V}{c} - \frac{1}{2\mu} \left(\frac{\partial P}{\partial y} + \rho g \right) c, \tag{44}$$

and the y -component of velocity is

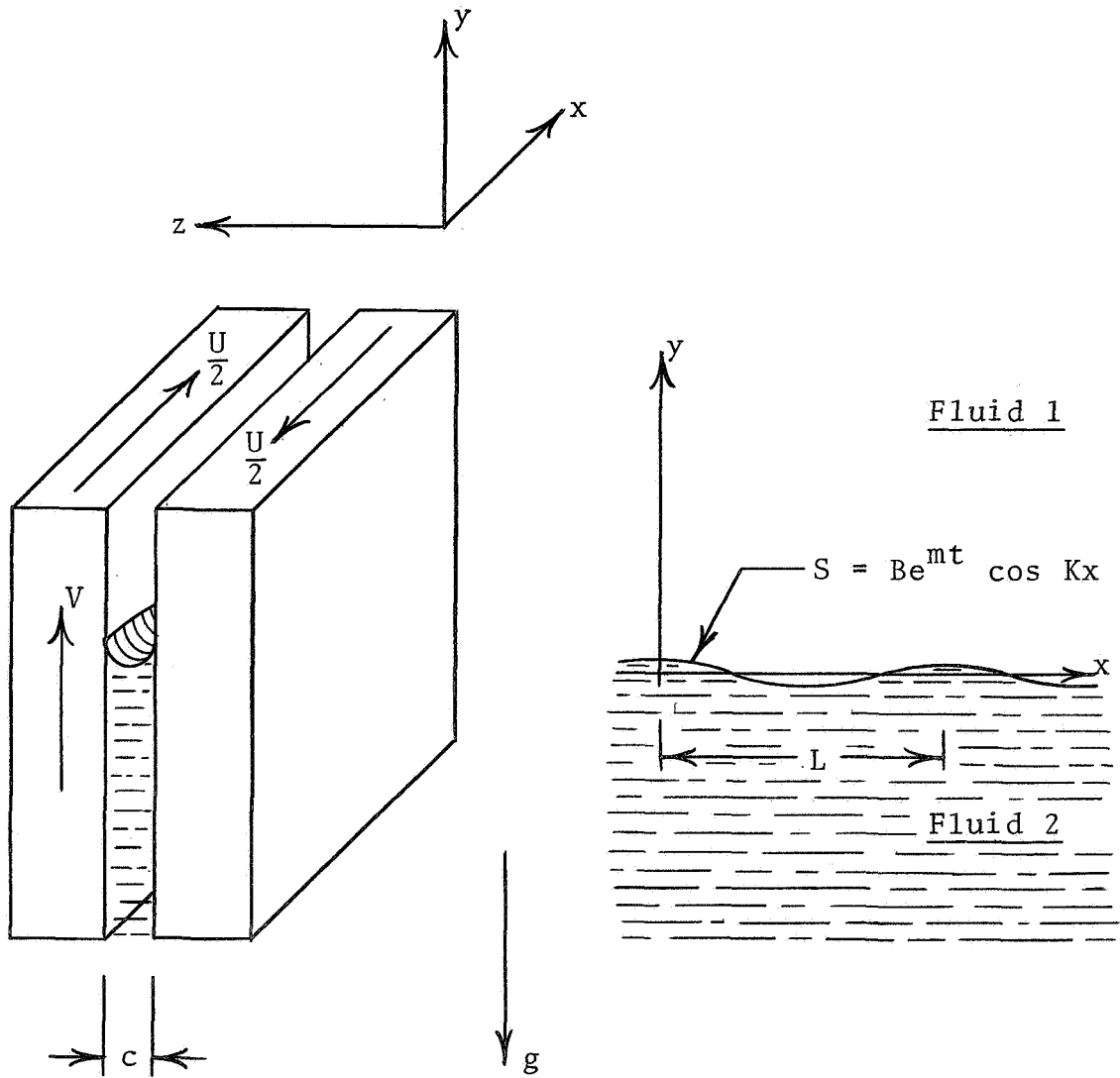


Figure 5. Model for analysis of a disturbed interface separating two viscous fluids moving transverse to the interface and confined between parallel plates having relative motion not parallel to the interface.

$$v = \frac{1}{2\mu} \left(\frac{\partial P}{\partial y} + \rho g \right) z^2 + \left[\frac{V}{c} - \frac{c}{2\mu} \left(\frac{\partial P}{\partial y} + \rho g \right) \right] z. \quad (45)$$

Substituting equation (45) into equation (18) and integrating yields the average velocity,

$$\bar{v} = - \frac{c^2}{12\mu} \left(\frac{\partial P}{\partial y} + \rho g \right) + \frac{V}{2} = \frac{\partial \phi}{\partial y}. \quad (46)$$

When equation (46) is integrated with respect to y , the solutions obtained for the pressures are

$$P_1 = - \frac{12\mu_1}{c} \left(\phi_1 - \frac{Vy}{2} \right) - \rho_1 gy + C_7, \quad (47)$$

and

$$P_2 = - \frac{12\mu_2}{c} \left(\phi_2 - \frac{Vy}{2} \right) - \rho_2 gy + C_8. \quad (48)$$

Equating the difference between the pressures from equations (47) and (48) with the pressure difference across the interface as given by equation (34), noting that constant terms are eliminated as given in equation (39), dividing by S and multiplying through by $K = 2\pi/L$ gives finally,

$$\begin{aligned}
& \frac{12m}{c^2} (\mu_1 e^{-KS} + \mu_2 e^{+KS}) \\
& = \frac{2\pi}{L} \left[\frac{12}{c^2} (\bar{v} - \frac{V}{2}) (\mu_1 - \mu_2) + (\rho_1 - \rho_2) g \right] \\
& \quad - \frac{8\pi^3 T}{L^3} . \tag{49}
\end{aligned}$$

Equation (49) differs from equation (40) only in the coefficient of the viscosity difference. Other things being equal, if both the interface velocity and the plate velocity were directed toward the more viscous fluid, a larger magnitude of interface velocity would be required to cause the interface to be unstable to a small disturbance than would be required when neither plate moves vertically. If, for example, the vertical velocity of the plate and the interface velocity were equal and both moving toward the more viscous fluid, the value of interface velocity necessary to cause an instability would be twice the value required with neither plate moving vertically. Therefore, the physical model would have a greater tendency toward instability of the interface when both runout and eccentricity are present simultaneously.

In assuming a pressure difference across the interface due to surface tension, to arrive at equation (34), it was assumed that P_1 was greater than P_2 , and that the interface was concave upward. If the interface were concave

downward, the pressure difference would be given by

$$(P_2 - P_1) = T \left(\frac{1}{R_1} + \frac{1}{R_2} \right), \quad (50)$$

where R_1 and R_2 are radii of curvature having centers below the interface instead of above it, as assumed in obtaining equation (34). But the curvature, as approximated by $\partial^2 S / \partial x^2$, is positive when the center of curvature is above the interface. Therefore, in establishing a sign convention for a center of curvature located below the interface, the curvature is approximated by

$$\frac{1}{R_2} = - \frac{\partial^2 S}{\partial x^2}, \quad (51)$$

and equation (50) becomes

$$(P_2 - P_1) = T \left(\frac{2}{c} - \frac{\partial^2 S}{\partial x^2} \right), \quad (52)$$

or

$$(P_1 - P_2) = T \left(-\frac{2}{c} + \frac{\partial^2 S}{\partial x^2} \right) \quad (53)$$

$$= T \left(-\frac{2}{c} - BK^2 e^{mt} \cos Kx \right). \quad (54)$$

The only difference between equation (54) and equation (37) is the algebraic sign on the constant term, which contains the clearance. But this term drops out

upon evaluation of the constants in the equations for the velocities. Therefore, the results are unchanged.

For a gas-liquid interface in which the liquid is completely non-wetting, and the angle of contact is 180 degrees, the conclusions concerning stability are identical to the conclusions reached for a liquid which wets the solid surfaces.

III. STABILITY ANALYSIS - ACCELERATION EFFECTS

The mathematical model for the analysis taking into account acceleration effects is shown in Figure 6. Viscous effects are neglected here and it is assumed that the fluid system undergoes an acceleration a normal to the interface and considered to be positive when directed downward, as shown in Figure 6.

The coordinate system is assumed to move with the bulk fluid motion. Effectively, slip flow is assumed, and the distance separating the plates enters into the mathematical analysis only in the pressure difference across the interface, but does not appear in the final result. The initial mathematical formulation is essentially the same as that presented by Taylor [11].

The interface is assumed to have a small wave-like perturbation, with the equation of the surface of separation given by

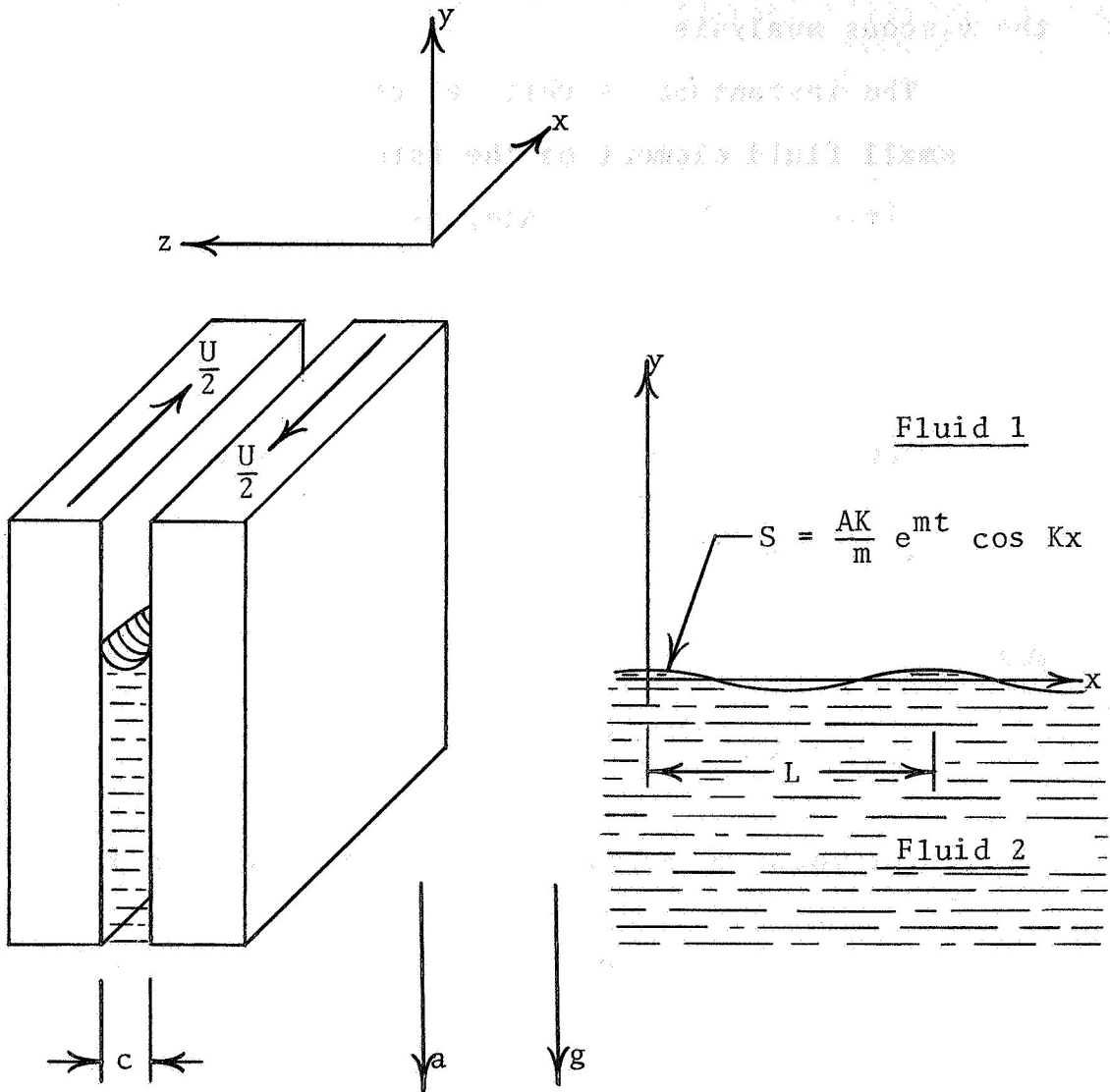


Figure 6. Model for analysis of the stability of an accelerated interface separating two fluids having different densities.

$$S = \frac{AK}{m} e^{mt} \cos Kx. \quad (55)$$

The disturbance will be unstable when m is positive, and the mathematical procedure is similar to that followed in the viscous analysis.

The instantaneous vertical component of the velocity of a small fluid element on the interface, relative to the mean position of the interface, is

$$v = \frac{\partial S}{\partial t} = AK e^{mt} \cos Kx. \quad (56)$$

The appropriate velocity potentials are

$$\phi_1 = - A e^{mt} - Ky \cos Kx, \quad (57)$$

and

$$\phi_2 = + A e^{mt} + Ky \cos Kx. \quad (58)$$

The equation of motion in the y -direction is

$$\frac{\partial P}{\partial y} = \rho(a - g - \frac{DV}{Dt}) \quad (59)$$

$$= \rho(a - g - \frac{\partial v}{\partial t} - u \frac{\partial v}{\partial x} - v \frac{\partial v}{\partial y}). \quad (60)$$

The inertia terms are obtained from the velocity potentials in equation (57) by taking the appropriate partial derivatives, which are,

$$u_1 = \frac{\partial \phi_1}{\partial x} = KA e^{mt} - Ky \sin Kx, \quad (61)$$

$$v_1 = \frac{\partial \phi_1}{\partial y} = KA e^{mt} - Ky \cos Kx, \quad (62)$$

$$\frac{\partial v_1}{\partial x} = -K^2 A e^{mt} - Ky \sin Kx, \quad (63)$$

$$\frac{\partial v_1}{\partial y} = -K^2 A e^{mt} - Ky \cos Kx, \quad (64)$$

$$\frac{\partial v_1}{\partial t} = mKA e^{mt} - Ky \cos Kx. \quad (65)$$

Equation (59) becomes, for fluid 1,

$$\frac{\partial P_1}{\partial y} = \rho_1 (a - g - mKA e^{mt} - Ky \cos Kx + Ku_1^2 + Kv_1^2). \quad (66)$$

For fluid 2, the required derivatives of the velocity potential are

$$u_2 = \frac{\partial \phi_2}{\partial x} = -KA e^{mt} + Ky \sin Kx, \quad (67)$$

$$v_2 = \frac{\partial \phi_2}{\partial y} = KA e^{mt} + Ky \cos Kx, \quad (68)$$

$$\frac{\partial v_2}{\partial x} = -K^2 A e^{mt} + Ky \sin Kx, \quad (69)$$

$$\frac{\partial v_2}{\partial y} = K^2 A e^{mt} + Ky \cos Kx, \quad (70)$$

$$\frac{\partial v_2}{\partial t} = mKA e^{mt} + Ky \cos Kx. \quad (71)$$

The equation of motion for fluid 2 becomes

$$\frac{\partial P_2}{\partial y} = \rho_2 (a - g - mKA e^{mt} + Ky \cos Kx - Ku_2^2 - Kv_2^2). \quad (72)$$

Neglecting squares of the disturbance velocities in equations (66) and (72) and integrating, the solutions for the pressures are,

$$P_1 = \rho_1 (a - g)y + \rho_1 mA e^{mt} - Ky \cos Kx + C_9, \quad (73)$$

and

$$P_2 = \rho_2(a - g)y - \rho_2 mA e^{mt} + Ky \cos Kx. \quad (74)$$

Assuming that the pressure difference across the interface, as given by equation (37),

$$(P_1 - P_2) = T \left(\frac{2}{c} + \frac{\partial^2 S}{\partial x^2} \right), \quad (37)$$

is applicable here, and setting equation (37) equal to the pressure difference obtained by subtracting equation (74) from equation (73), gives

$$\begin{aligned} T \left(\frac{2}{c} - \frac{AK^3}{m} e^{mt} \cos Kx \right) &= (\rho_1 - \rho_2)(a - g)S \\ &+ mA e^{mt} (\rho_1 e^{-KS} + \rho_2 e^{+KS}) \cos Kx \\ &+ (C_9 - C_{10}). \end{aligned} \quad (75)$$

When $\cos Kx$ is zero, S is zero, and equation (75) reduces to

$$\frac{2T}{c} = (C_9 - C_{10}). \quad (76)$$

When equation (75) is divided through by S , as given by equation (55), equation (75) becomes

$$\frac{m^2}{K} (\rho_1 e^{-KS} + \rho_2 e^{+KS}) = (a - g)(\rho_2 - \rho_1) - TK^2. \quad (77)$$

The algebraic sign of \underline{m}^2 is the same as the right-hand side of equation (77). If \underline{m}^2 is negative, \underline{m} is imaginary and the amplitude of the disturbance varies sinusoidally with time. This reflects the fact that viscous forces were neglected in the analysis. When \underline{m}^2 is positive, the sign of \underline{m} could be either positive or negative, from a strictly mathematical standpoint. However, the omission of viscous forces in the analysis removes any means of damping, and it is therefore concluded from purely physical considerations that \underline{m} will be positive when \underline{m}^2 is positive and the disturbance will increase exponentially with time until it attains an amplitude which is no longer small compared with the wavelength.

When the gravitational acceleration acts toward the more dense fluid, equation (77) predicts that an instability will result from an acceleration of the fluid system toward the more dense fluid at a value which is sufficiently larger than gravity to cause the first term on the right to be larger than the second term. Therefore, surface tension contributes toward stability of the interface.

The minimum wavelength of an unstable disturbance can be found from equation (77). The substitution $K = 2\pi/L$, where L is the wavelength of a disturbance, is made in equation (77).

Unstable disturbances, having a wavelength L_u , exist only when the right-hand side of equation (77) is greater than zero. Stated mathematically,

$$(a - g)(\rho_2 - \rho_1) - \frac{4\pi^2 T}{L_u} > 0. \quad (78)$$

When equation (78) is solved for L_u , the effect of surface tension is found to be to restrict unstable disturbances to those of wavelength greater than a critical value, given by

$$L_u > \frac{2\pi T^{1/2}}{(a - g)(\rho_2 - \rho_1)}. \quad (79)$$

Upon reaching a finite value, the amplitude of unstable disturbances will continue to grow and will result in the formation of fingers. The supporting reasoning is similar to that given for the growth of the unstable disturbances of the interface between the viscous fluids of Figure 4, page 21, into fingers.

The model shown in Figure 4 is also applicable to an unstable interface in an accelerated fluid system. Considering a gas-liquid interface, and ignoring the density of the gas, the interface pressure may be assumed constant. When the system is being accelerated toward the more dense fluid, the liquid in this case, the pressure in the liquid

at a location which is several wavelengths from the interface will be dependent only on the distance from the mean position of the interface. But at positions in the neighborhood of the interface, the pressure gradient near the leading portion of the interface will be greater than the pressure gradient near the lagging portion. Hence, the acceleration of the fluid near the leading portion will be greater in magnitude, and its velocity will become increasingly larger than the velocity of the fluid near the lagging portion. Thus, the amplitude of the disturbance will continue to grow.

In an annulus between rotating cylinders, accelerations normal to the interface occur due to eccentricity and runout. Since the acceleration is alternately positive and negative, the wavelength of the fingers and the length to which fingers would grow would depend on the magnitude of eccentricity and runout, surface tension, shaft speed, etc., and would determine the potential for trapping gas bubbles in the liquid.

CHAPTER III

EXPERIMENTAL STUDY

I. EXPERIMENTAL FACILITY

The test facility was designed and built to permit visual observations and photographic recording of an interface separating air and a liquid confined in the annular space between a rotating cylinder and a stationary housing.

A transparent cylindrical housing is mounted to the test frame, as shown in Figure 7. Housings having nominal inside diameters of two, four, six or eight inches can be accommodated. Glass, and transparent acrylic plastic housings were used in the experimental work. An O-ring seal was used between the housing and the base.

The stainless steel shaft, which is driven through a V-belt by a variable speed motor, was designed for mounting interchangeable test rotors ranging from two to eight inches in diameter. The test rotors, which were made of aluminum, have a length of six inches. The rotors are positioned on the shaft by a tapered shoulder on the shaft, and a tapered nut at the lower end. The rotors were ground and polished, and the runout was about 0.0003 to 0.0010 inch.

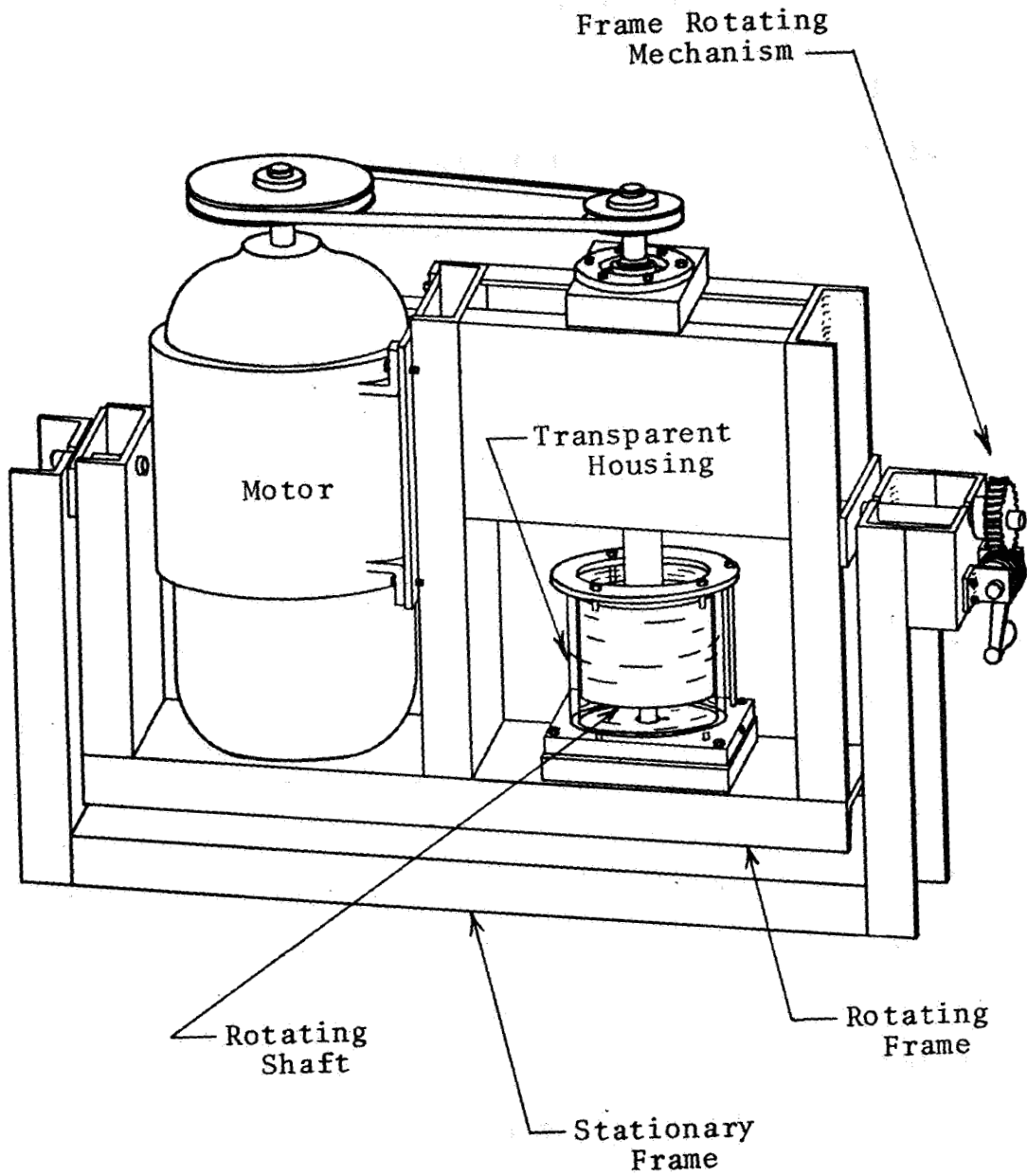


Figure 7. Interface study facility.

The shaft is supported by a ball bearing at the end on which the V-belt sheave is mounted. A helical groove hydrodynamic journal bearing having a diameter of one inch supports the other end, and is lubricated by the liquid being used in the interface study.

Provision was made for rotating the test frame through an angle of 180 degrees, in order to attain any desired angle of orientation of the shaft axis in the gravitational field.

With the frame orientation as shown in Figure 7, the volume below the test rotor, and within the housing, is the liquid reservoir. A hole was drilled and tapped in the base, and a valve was fitted into the passage to permit liquid to be introduced into the reservoir from below. This arrangement makes it possible to exclude all air bubbles from the reservoir by filling it through this passage. The annulus is open to the atmosphere at the top of the rotor.

A view of the test rig after completion of construction is shown in Figure 8. The housing mounted in the test rig in this view is a five-inch outside diameter acrylic cylinder with an inside diameter of 4.116 inches. The aluminum rotor mounted on the shaft has a diameter of 3.990 inches. In the left background of Figure 8 are other rotors having a nominal diameter of four inches, and also

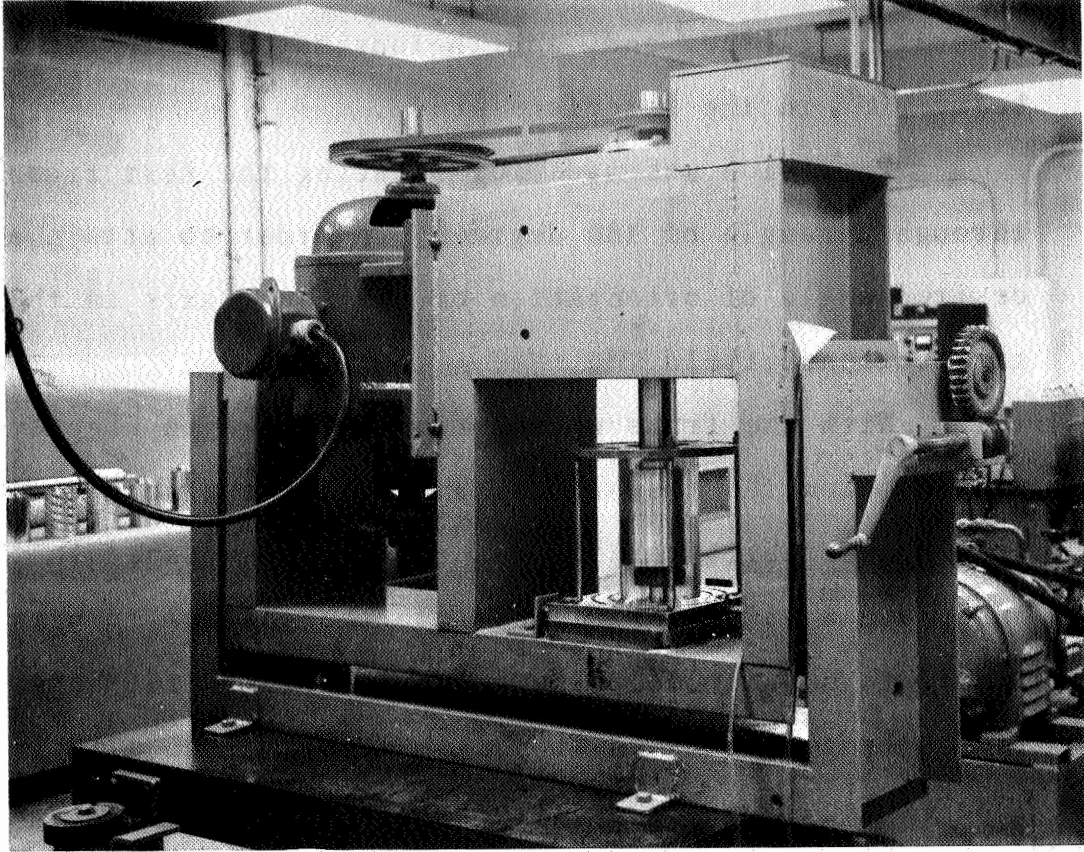


Figure 8. Experimental facilities.

an extra shaft. The threaded rotors were used in viscoseal performance tests in a companion study. The white plastic funnel is attached to plastic tubing, which connects to the valve through which the reservoir is filled with liquid. In Figure 8, distilled water is in the reservoir, and the interface level is about midway up on the aluminum rotor.

No provision was made for cooling the working fluid. However, a thermocouple was installed in a radial hole drilled through the acrylic cylinder to provide for monitoring the temperature of the liquid in the annulus.

Visual observations were facilitated by the use of a stroboscope, which was also used as the light source for still photographs of about 1.2 microseconds exposure time. The still photographs were made with a 35 mm camera using black and white film.

High speed movies were made at film speeds up to 5,000 frames per second using black and white film. Illumination was provided by two lamps, each having a rating of 1,000 watts.

II. DESCRIPTION OF EXPERIMENTAL INVESTIGATION

An annulus with a nominal diameter of four inches was arbitrarily chosen for the initial experimental studies, which preceded the analytical development presented in

Chapter II. Because of the nature of the subsequent analytical development, it was not found necessary to employ the full range of diameters for which the facility was designed. Consequently, annuli with a nominal diameter of four inches, but with a variation in the thickness, were employed throughout the experimental study.

Three radial clearances were used in the experimental work. Specific dimensions of the rotor-housing combinations are given in Table I.

TABLE I.
DIMENSIONS OF ROTOR-HOUSING COMBINATIONS
USED IN THE EXPERIMENTAL WORK

<u>Rotor Diameter (Inches)</u>	<u>Housing I.D. (Inches)</u>	<u>Avg. Radial Clearance (Inches)</u>
3.990	4.002	0.006
3.980	4.002	0.011
3.990	4.116	0.063

A 0.006-inch average radial clearance was provided by two different housings, one made of glass and one made of acrylic, and each having an inside diameter of 4.002 inches.

In the early experimental work, which was of an exploratory nature, air bubbles were observed to be present in the annulus at sufficiently high shaft speeds. An effort

was made to establish an empirical criterion for the onset of air entrainment. Following the approach taken by McGrew and McHugh [5], and by King [6], the Reynolds number and the Weber number were considered in attempting to obtain a correlation with the beginning of air entrainment.

Studies were made at shaft speeds up to 4,000 rpm using fluids having viscosities from 0.5 centipoise for methyl alcohol up to 1200 centipoise for glycerine. Values of surface tension for the fluids employed ranged from 22 dynes/cm. for ethyl alcohol to 72 dynes/cm. for water. No significant relation was established between the beginning of air entrainment and the Weber number or Reynolds number, or combination of the two numbers. However, it was found that air entrainment occurred for some fluids, particularly the more viscous fluids, under laminar flow conditions. For a Reynolds number based on the surface velocity of the rotor and on the radial clearance, Couette flow remains laminar for Reynolds numbers below 1,000 [14], and may remain laminar at Reynolds numbers of four times this value [15]. Air entrainment was observed to occur at Reynolds numbers of 100 or less, placing the flow well into the laminar regime.

The observation that air entrainment could occur under laminar flow conditions, as well as under turbulent flow conditions, provided insight as to the general direction

which the analytical study should take. This eventually led to the theoretical prediction of an interface instability not closely related to either the Reynolds number or the Weber number.

Experimental verification of the predicted instability of the interface was primarily of a qualitative nature only. While the runout and eccentricity in the experimental facility provided the conditions to produce an interface instability, they also presented problems in determining local velocities and radial clearances.

However, visual observation revealed an oscillating interface, and by varying the shaft speed and the viscosity of the liquid used, conditions could be produced which would cause the formation of fingers of air extending into the liquid. These fingers were seen with the aid of a stroboscope, and air bubbles trapped below the interface were also seen. But the actual development of the fingers and the trapping of the air bubbles were not seen satisfactorily, except at very low shaft speeds.

For the higher shaft speeds, a high-speed movie camera was used to facilitate viewing the development of fingers and the formation of air bubbles. Film speeds up to 5,000 frames per second were used for shaft speeds up to 2140 rpm.

CHAPTER IV

EXPERIMENTAL RESULTS

Air entrainment occurred with each of the three clearances employed in the experimental study. The shaft speed at which air entrainment occurred varied with the thickness of the annulus, and with the properties of the liquid being used.

Clearance of 0.006 inch

The results obtained with a glass housing providing a clearance of 0.006 inch were not identical to the results obtained with an acrylic housing providing the same clearance, but the difference in the results was not attributed to the difference in the materials of which the housings were made. There were differences of comparable magnitude between different test runs using the same acrylic housing. The differences were attributed primarily to unavoidable variations in runout and eccentricity. These variations were created when the apparatus was disassembled for cleaning, or other purposes, and then reassembled with a slightly different alignment of rotor and housing.

The eccentricity ratio, which could not be precisely determined, was estimated to be about 0.1 to 0.4 for tests

conducted with the glass housing and with the acrylic housing.

Using a 50% glycerine and 50% water solution, having a viscosity of five centipoise at room temperature, the formation of pronounced fingers was observed at relatively low shaft speeds. The photograph shown in Figure 9 was taken when the shaft speed was 50 rpm. The corresponding Reynolds number was eight, indicating the presence of laminar flow conditions. This photograph depicts a typical interface profile with pronounced fingers formed under the influence of viscous effects.

Using the same solution, a few hundred feet of 16 millimeter movie film were taken for shaft speeds up to 600 rpm. The progressive stages of the development of the fingers can be seen on this film. A typical movie film sequence is shown in Figure 10 for a shaft speed of 440 rpm.

Interface details were not easily discernible when viewing the motion picture projected at normal speeds, and were quite difficult to see in single frame viewing. For this reason, the same film sequence is reproduced as Figure 11, where the interface has been traced with ink on the photographic prints in order to assist in visually following the changes in the interface seen in the unaltered photograph of Figure 10.

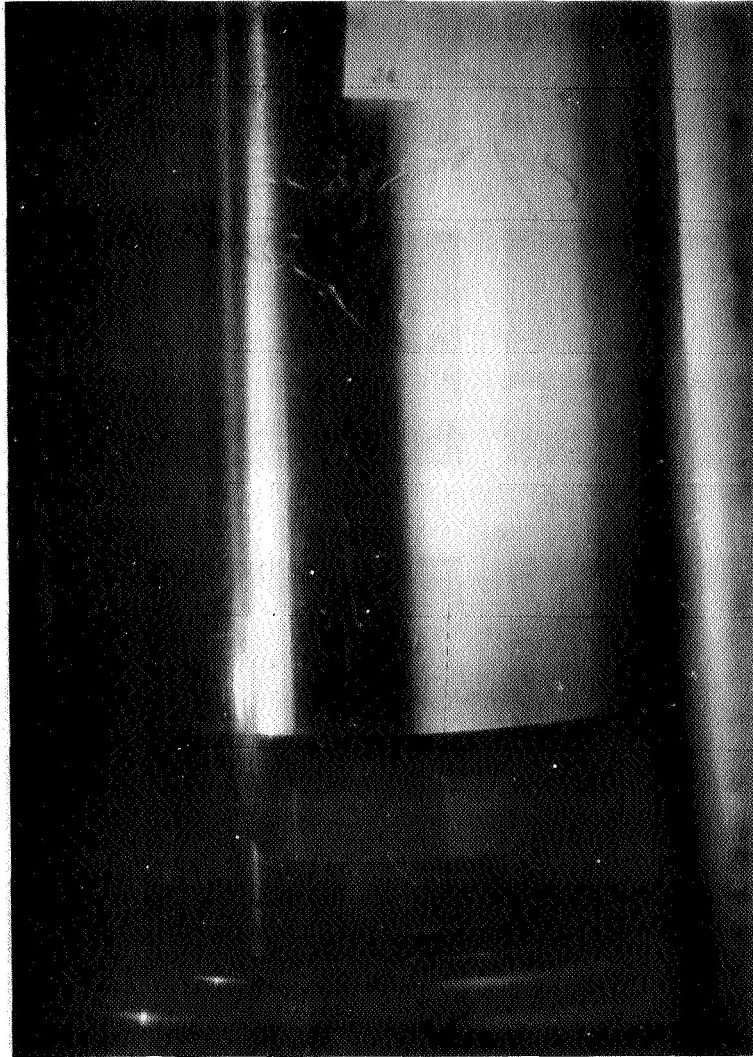


Figure 9. Fingers of air and 50% mixture of glycerine and water at shaft speed of 50 rpm.

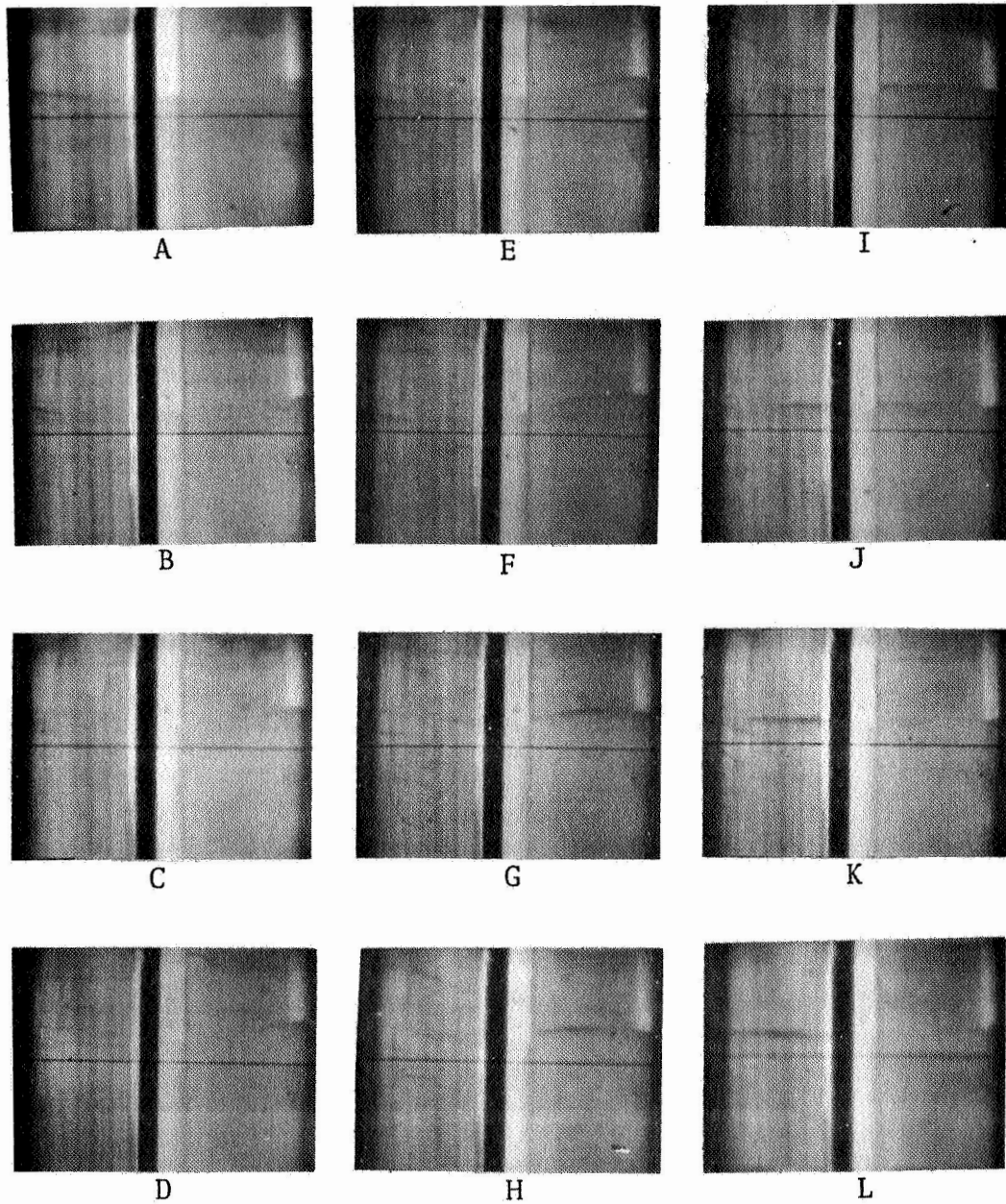


Figure 10. Motion picture frame sequence showing development of fingers in 50% glycerine-50% water solution. Shaft rotation of 26.5° between frames, shaft speed - 440 rpm, clearance - 0.006 inch.

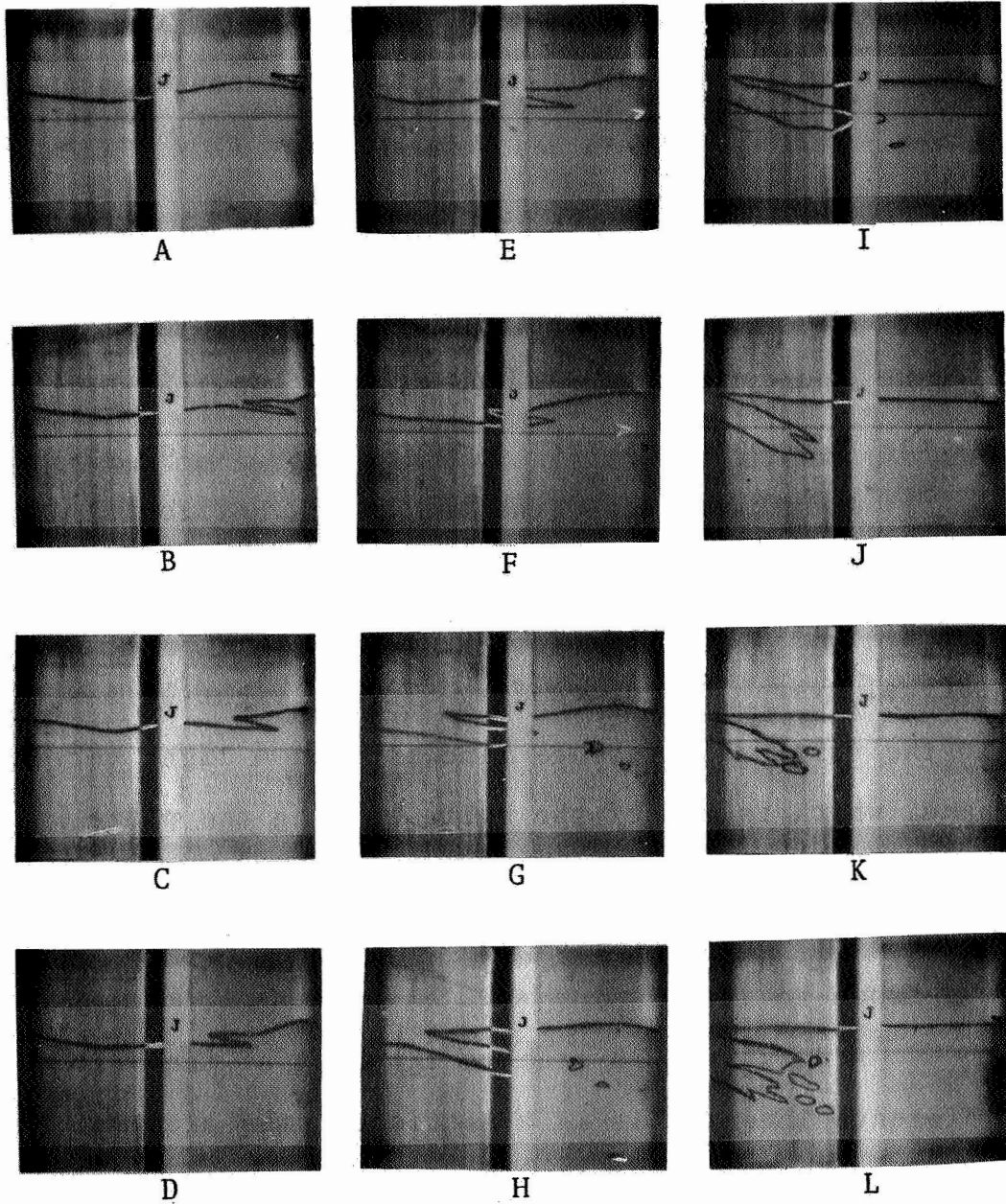


Figure 11. Retouched motion picture frame sequence showing development of fingers in 50% glycerine-50% water solution. Shaft rotation of 26.5° between frames, shaft speed - 440 rpm, clearance - 0.006 inches.

The film speed for the movie sequence shown was 500 frames per second, and every fifth frame of the film is shown in Figures 10 and 11. Elapsed time between adjacent frames shown was 0.01 second, representing the time for 26.5 degrees of shaft revolution.

The interface was descending in the first nine or ten frames shown. This is not immediately apparent in the photographs shown, but was readily seen in viewing the projection of the film onto a screen at normal projection speeds.

A dark vertical line and a dark horizontal line, each passing through the center of the picture, are seen in each frame. These reference lines were built into the optical system of the camera. To the right of and adjacent to the vertical reference line is seen a light vertical band, which is one of the bolts holding the plate which clamps the transparent housing into position. The bolt was wrapped with white paper, and a film identification number was taped to it.

A dark band is seen to the left of the vertical reference line. This is a section of the aluminum rotor which was insufficiently lighted because of the difficulty in uniformly illuminating a curved, highly reflective surface.

When using distilled water in the annulus, severe gas ingestion generally occurred at shaft speeds above

2150 rpm, and interface irregularities were observed at shaft speeds above 1100 to 1350 rpm. The variation in minimum speed at which these irregularities became evident was attributed to the unavoidable differences in eccentricity and runout previously discussed.

On one occasion, with the shaft operating at 1100 rpm, the interface showed no irregularities and no trapped air bubbles were visible. As the shaft continued to operate at 1100 rpm, the shaft axis was rotated 180 degrees, placing the liquid above the interface and the air below it. The shaft continued to operate at this speed, with the interface inverted, for over an hour with no visible evidence of air bubbles in the liquid or any loss of liquid from the interface.

However, on another occasion, when the shaft eccentricity was probably different, interruptions of the interface and air ingestion occurred for the same shaft speed with the shaft oriented in the normal position (interface not inverted). This is shown in Figure 12.

A comparison of Figure 12 with Figure 9, page 49, indicates interface irregularities and trapped air bubbles of smaller dimensions at the higher shaft speed. Although viscous effects and acceleration effects on the interface were present simultaneously, the viscosity of the water in Figure 12 was only 20 per cent of the viscosity of the

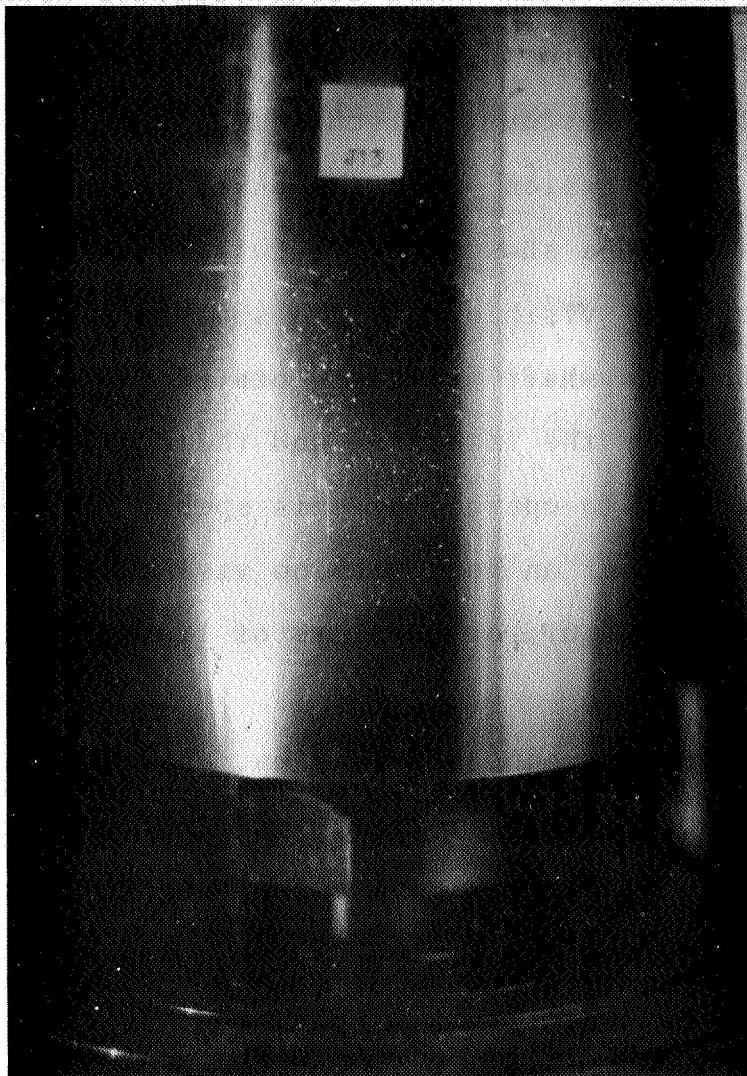


Figure 12. Air-distilled water interface region at shaft speed of 1100 rpm.

glycerine-water solution in Figure 9 and suggests a stronger influence of acceleration effects on the air entrainment in Figure 12.

Clearance of 0.011 inch

The eccentricity ratio was estimated to be less than 0.2 for observations made with a clearance of 0.011 inch.

Using water in the annulus, air bubbles were present in the annulus for shaft speeds above 1100 rpm.

The shaft axis was rotated 180 degrees while the shaft was operating, and no leakage from the interface was observed.

Clearance of 0.063 inch

An eccentricity ratio of less than 0.1 was estimated for a clearance of 0.063 inch.

Using water in the annulus, air bubbles appeared in the annulus at shaft speeds of 670 rpm or higher. The bubbles were observed to be aligned in circumferential rows with an axial spacing varying from about 0.15 inch at low speeds up to about 0.25 inch at speeds above 3000 rpm.

The rows of bubbles had not been anticipated, and aluminum powder was mixed with the water in the annulus in order to verify that the spacing of the rows of bubbles corresponded to the spacing of vortex pairs predicted by

Taylor [16]. The initiation, theoretically and experimentally, of the Taylor instability was found to be 25 rpm. With increased shaft speed, the axial spacing of the Taylor's vortex pairs was found to increase from the 0.125-inch spacing predicted by Taylor for the onset of the instability.

Efforts to operate the shaft in the inverted position without the loss of water were unsuccessful. A large range of shaft speeds was employed in attempts to rotate the shaft axis, while the shaft was rotating, without a breakup of the interface. In all efforts, water was lost from the annulus before the shaft axis was rotated through an angle of more than about 120 degrees.

CHAPTER V

DISCUSSION

The theoretical development presented in Chapter II and experimentally verified in a qualitative way, with typical results displayed in Chapter IV, provides an explanation of a possible mechanism by which gas ingestion can occur in the region of a gas-liquid interface.

The operation of a viscoseal involves regions in which the interface has a component of velocity relative to one of the surfaces such that the liquid is advancing on a solid surface, and other regions where the interface is receding on the solid surface. With runout of the rotating shaft, there may be regions in which the liquid is receding on both surfaces. An interface which is receding on one or both surfaces may be subject to the viscous type of interface instability, which could lead to gas entrainment.

Fluid particles adjacent to the interface in the viscoseal are also subjected to local accelerations having a component normal to the interface. These normal acceleration components, when directed toward the liquid, can also cause an interface instability resulting in gas entrainment.

The subsequent motion of gas bubbles thus trapped would depend on a number of variables, including the orientation of the viscoseal in the gravitational field, the

viscoseal geometry, whether turbulence exists, and other factors. If all entrained bubbles subsequently moved back to the interface rather than being transported away from the interface, the effect of the gas entrainment could be inconsequential with respect to the satisfactory operation of the viscoseal. However, if entrained gas bubbles continually accumulate in the liquid confined in the annular space, the viscoseal would most frequently be rendered ineffective to its intended purpose. As discussed in Chapter I, the mechanics of the gas transport process is a separate aspect of the problem associated with gas ingestion, and is not well understood.

In the viscoseal, a small element of fluid adjacent to the interface has motion with respect to the grooved surface as well as having motion with respect to the smooth surface. An unstable disturbance, in the form of a developing finger, will have the same general motion as the local average motion of the liquid element in which the disturbance is located. An undetermined but finite amount of time is required for a small disturbance to grow to a sufficient size to result in the joining of the tips of two liquid fingers to isolate a quantity of gas as a bubble. If, during the time of growth of such a disturbance, the liquid element and its developing disturbance move into a region which is stable to a small perturbation, then

the disturbance will no longer continue to grow, but will begin to decrease in size and no gas bubble will have resulted from the disturbance.

Therefore, the theory presented here does not lead to a quantitative prediction of the actual trapping of a gas bubble in the liquid. Thus regimes of viscoseal operation in which gas ingestion would be expected could not be determined, even if the motion of the fluid field were known.

However, if the fluid motion were known, operating ranges which could be definitely expected to be free of gas ingestion could be established by determining that interface stability existed on all parts of the interface during the entire time of one shaft revolution. This assumes that there are no mechanisms of gas ingestion other than those presented here.

Other physical applications approximately fitting the hypothetical model include face seals, buffered bushing seals, and journal bearings.

Journal bearings are inherently vulnerable to gas entrainment resulting from the type of interface instability presented here, since any radial load results in eccentric operation of the journal. If the bearing is not immersed in the lubricant, and a gas-liquid interface exists in the annulus, then over a portion of the interface the liquid is receding from the solid surface of the shaft. This

application represents rather closely the model on which the analytical study was based, and the journal bearing operation is essentially identical to the experimental facility used in the interface stability study. However, cavitation (where the local pressure becomes less than the vapor pressure of the lubricant) could occur in the annulus of a journal bearing which is completely immersed and involves a different mechanism than that causing what is referred to here as gas ingestion.

Buffered bushing seals are similar in many respects to the journal bearing, and gas ingestion encountered in the buffered bushing seal may well have its origin in the same type of interface instability which is postulated here to occur in the journal bearing.

Face seals represent, ideally, relative motion between two closely spaced parallel plates between which a gas-liquid interface exists. Due to non-uniformity of the spacing between the plates, the interface would not have the shape of a circle and the distance from the interface to the center of rotation would vary along the interface. Therefore, a receding interface would exist in a region or regions, and fluid elements in the interface would also undergo normal accelerations. Hence, potential conditions for instability of the interface and for gas ingestion are present. The potential for gas ingestion would appear to be considerably

greater when sealing a liquid in the center from a gas, since the centrifugal acceleration of the interface is directed toward the liquid.

Helically-grooved face seals have characteristics similar to the viscoseal, in that the fluid flow in the vicinity of the interface is considerably complicated by the presence of the grooves and lands. Those designed for inward pumping of the liquid would appear to have a greater tendency toward gas ingestion than face seals with plain surfaces.

The results in the experimental work were frequently not satisfactorily reproducible. As discussed earlier, some of the variations in results were attributed to differences in shaft and housing alignment. However, there were also occasions when there was no reason to believe that there were changes in dimensions of the physical equipment, and yet the gas ingestion characteristics varied substantially from one observation to another. These variations were particularly noticeable when there was a time interval of several hours between an observed event and an attempt to duplicate the event.

The mathematical model on which the theoretical development was based was considerably simplified in order to permit an analytical solution. A contact angle of zero was assumed in order to determine an expression for the

pressure difference across the interface. It was noted in Chapter II that the mathematical result is unchanged by assuming a non-wetting interface, and it is seen that for any uniformly constant interface contact angle the mathematical results are unchanged.

However, Dettre and Johnson [13] have shown that advancing and receding contact angles may differ by as much as 80 degrees. Also, nonuniformity of the surface causes local variations in contact angles. These authors also imply that the relative humidity of the air in contact with an air-liquid interface affects the angle of contact, and the time of exposure of a liquid to a surface is stated to influence the contact angle.

In the experimental work reported here, the relative humidity of the air in the laboratory was not controlled, nor was it recorded. Also, changes in the physical appearance of the surface of the aluminum rotors were observed, causing speculation that oxidation or other changes were producing changes in the wetting characteristics on the surface.

One particular variation in properties observed to result from long time intervals between experimental observations was the composition of mixtures of glycerine and water, with the attendant variations in viscosity and other properties. It was discovered that the amount of water in

solution increases or decreases significantly when the solution is not in equilibrium with the air to which the liquid surface is exposed. Then after equilibrium is reached, measurable changes in composition occur from one day to the next as the relative humidity of the air increases or decreases. The room temperature was held within a narrow range, winter and summer, but the relative humidity was not.

These factors are pointed out to indicate some of the variables which may enter into the problem of obtaining reproducible results in visco seal operation, or other related applications.

Although the problem of reproducibility was experienced in this work, the problem did not prevent the achievement of the objective of the tests - that of verifying the mechanism by which gas ingestion can occur in an interface between rotating cylinders.

CHAPTER VI

CONCLUSIONS AND RECOMMENDATIONS

Some conclusions evolving from this investigation are that:

1. A phenomenological explanation of gas ingestion can be obtained through a stability analysis of a dynamic gas-liquid interface.

2. For fluids contained between closely spaced surfaces, gas ingestion can be caused by a gas-liquid interface instability resulting from a velocity and/or an acceleration of the interface toward the liquid.

3. Surface tension tends to prevent interface instabilities and gas ingestion.

4. Gas ingestion in viscoseals appears to be an essentially inherent phenomenon which can not be readily eliminated through optimization of the geometry.

5. Eccentricity, shaft runout and vibrations contribute to conditions necessary for the instability of an interface in rotating machinery.

Although a mechanism of gas ingestion has been established, both theoretically and experimentally, this study did not provide a quantitative criterion for predicting gas ingestion. For specific engineering applications

in which a gas-liquid interface must be present in an annulus between rotating shafts, information is needed to aid in selecting design parameters which will provide operation free of the problem of gas ingestion.

Since gas ingestion in viscoseals seems to be a phenomenon which is not easily avoided, efforts should be made to design a method of separating out the ingested gas. A substantial effort in this direction has been reported by Boon [17]. A further effort to provide a recirculation and centrifugal separation path in the viscoseal is being made by the Mechanical and Aerospace Engineering Department at The University of Tennessee.

BIBLIOGRAPHY

BIBLIOGRAPHY

1. Lindau, J. W., III, "Extrusion Then and Now," *Plastics World*, Sept. 1968, pp. 50-55.
2. Lawaczeck, F., *Turbinen und Pumpen*, Springer Verlag, 1932.
3. Pearsall, R. H., "The Screw Oil Pump," *The Automobile Engineer*, May 1924, pp. 145-147.
4. Rowell, H. S., and Finlayson, D., "Screw Viscosity Pumps," *Engineering*, Vol. 126, Aug. 31, 1928, pp. 249-250, Sept. 28, 1928, pp. 385-387, and Discussion, Nov. 23, 1928, pp. 659-660.
5. McGrew, J. M., and McHugh, J. D., "Analysis and Test of the Screw Seal in Laminar and Turbulent Operation," *Trans. ASME, Series D*, Vol. 87, 1965, pp. 153-162.
6. King, Alan E., "Screw Type Shaft Seals for Potassium Lubricated Generators," *IEEE Trans. on Aerospace*, Vol. AS-3, June 1965 Supplement, pp. 471-479.
7. Stair, W. K., "Theoretical and Experimental Studies of Visco-Type Shaft Seals," *Mechanical and Aerospace Engineering Research Report ME 65-587-4*, University of Tennessee, October 20, 1965.
8. Stair, W. K., "Theoretical and Experimental Studies of Visco-Type Shaft Seals," *Mechanical and Aerospace Engineering Research Report ME 66-587-5*, University of Tennessee, April 28, 1966.
9. Ludwig, L. P., Strom, T. N., and Allen, G. P., "Gas Ingestion and Sealing Capacity of Helical Groove Fluid Film Seal (Viscoseal) using Sodium and Water as Sealed Fluids," *NASA TN D-3348*, NASA, Washington, D. C., March 1966.
10. Saffman, P. G., and Taylor, Sir Geoffrey, "The Penetration of a Fluid Into a Porous Medium or Hele-Shaw Cell Containing a More Viscous Liquid," *1958 Proc. Roy. Soc., A*, 245, pp. 312-341.

11. Taylor, Sir Geoffrey, "The Instability of Liquid Surfaces When Accelerated in a Direction Perpendicular to Their Planes, I," 1950 Proc. Roy. Soc., A, 201, pp. 192-196.
12. Lamb, Horace, Hydrodynamics, Dover, 1945, p. 456.
13. Dettre, R. H., and Johnson, R. E., "Contact Angle Hysteresis. IV. Contact Angle Measurements on Heterogeneous Surfaces," Journal of Physical Chemistry, Vol. 69, 1965, pp. 1507-15.
14. Pan, C. H. T., and Vohr, J. H., "Super-Laminar Flow in Bearings and Seals," Bearing and Seal Design in Nuclear Power Machinery, ASME, presented at The Symposium on Lubrication in Nuclear Applications, June 5-7, 1967, Miami Beach, Fla., pp. 219-245.
15. Schlichting, Hermann, Boundary Layer Theory, McGraw Hill, 1960, p. 440.
16. Taylor, G. I., "Stability of a Viscous Liquid Contained Between Two Rotating Cylinders," Philosophical Transactions, Series A, 223, 1923, pp. 289-343.
17. Boon, R. J. G., "Waarnemingen Aan Een Visco Afdichting In Een Transparant Huis," Afstudeerverslag, Technische Hogeschool Delft, June, 1968.

DISTRIBUTION LIST

Defense Documentation Center
Cameron Station
Alexandria, Virginia 22314

Mr. P. H. Broussard
NASA, R-ASTR-GC
Marshall Space Flight Center
Huntsville, Alabama 35812

Mr. John J. Gurtowski
Naval Air Systems Command
Code AIR 52032C - Dept. of the Navy
Washington, D. C. 20360

Mr. Robert L. Johnson
Chief, Lubrication Research Branch
NASA, Lewis Research Center
Cleveland, Ohio 44135

Mr. W. C. Karl
Office of Naval Research, Code 473
Department of the Navy
Washington, D. C. 20360

Mr. Lawrence P. Ludwig
Head, Seals Section
NASA, Lewis Research Center
Cleveland, Ohio 44135

Mr. Joseph Maltz
Materials Research Program
National Aeronautics & Space Adm.
Washington, D. C. 20546

Col. W. Metscher
Office of Director of Defense Research
and Engineering
Room 3C128, Pentagon
Washington, D. C. 20301

Mr. E. R. Taylor
Reactor Engineering Division
Oak Ridge National Laboratory
Oak Ridge, Tennessee 37830

Mr. Marshall J. Armstrong, Jr.
U. S. Army Mobility Equipment Research
and Development Center
Fort Belvoir, Virginia 22060

Mr. Richard N. Belt
U. S. Army Mobility Equipment Research
and Development Center
Fort Belvoir, Virginia 22060

Mr. Floyd Lux
U. S. Tank Automotive Center
Propulsion Systems Laboratory, SMOTA-RCP.4
Warren, Michigan 48090

Mr. J. R. Crowder
Flight Mechanics & Fluid Systems Section
(AIR 5303)
Naval Air Systems Command - Dept. of the Navy
Washington, D. C. 20360

Mr. Roy R. Peterson
Naval Ship Systems Command (Code 03413)
Department of the Navy
Washington, D. C. 20360

Dr. Earl Quandt
Naval Ship Research & Development Center
Annapolis Division
Annapolis, Maryland 21402

Mr. Alan Schrader
Naval Ship Research & Development Center
Annapolis Division
Annapolis, Maryland 21402

Mr. Lyman Carlyle Fisher
Naval Ordnance Laboratory
Department F (Code 510) - White Oak
Silver Spring, Maryland 20910

Mr. Stanley Doroff
Office of Naval Research (Code 438)
Department of the Navy
Washington, D. C. 20360

Mr. John W. Zmurk
Air Force Aero Propulsion Laboratory (APIP-1)
Wright-Patterson Air Force Base, Ohio 45433

Capt. Kenneth R. Hooks
Air Force Weapons Laboratory WLDC
Kirtland Air Force Base, New Mexico 87117

Dr. Joseph F. Masi
Air Force Office of Scientific Research, SREP
1400 Wilson Boulevard
Arlington, Virginia 22209

Mr. Frank J. Mollura
Rome Air Development Center, EMEAM
Griffiss Air Force Base, New York 13440

Mr. Gerald S. Leighton
SEPO - Division of Space Nuclear Systems
U. S. Atomic Energy Commission
Washington, D. C. 20545

Mr. C. E. Miller, Jr.
Division Reactor Development & Technology
U. S. Atomic Energy Commission
Washington, D. C. 20545

Bureau of Naval Personnel
Department of the Navy
Washington, D. C. 20370
Attn: Technical Library

Naval Air Systems Command
Department of the Navy
Washington, D. C. 20360
Attn: Technical Library Division, AIR-604

Naval Applied Science Laboratory
Flushing and Washington Avenues
Brooklyn, New York 11251
Attn: Technical Library, Code 222

U. S. Naval Oceanographic Office
Suitland, Maryland 20390
Attn: Library, Code 1640

U. S. Naval Postgraduate School
Monterey, California 93940
Attn: Library, Code 0212

DISTRIBUTION LIST (Cont'd)

Naval Ship Engineering Center
Philadelphia Division
Philadelphia, Pennsylvania 19112
Attn: Technical Library

Naval Ship Research & Development Center
Annapolis Division
Annapolis, Maryland 21402
Attn: Library, Code A214

Naval Ship Systems Command
Room 1532 Main Navy
Washington, D. C. 20360
Attn: Technical Library

U. S. Atomic Energy Commission
Argonne National Laboratory
9700 South Cass Avenue
Argonne, Illinois 60440
Attn: Library

National Bureau of Standards
Washington, D. C. 20025
Attn: Library

Battelle Memorial Institute
505 King Avenue
Columbus, Ohio 43201
Attn: Library

Massachusetts Institute of Technology
Cambridge, Massachusetts 02139
Attn: Library

Naval Undersea Warfare Center
3202 East Foothill Boulevard
Pasadena, California 91107
Attn: Technical Library

Navy Underwater Sound Laboratory
Fort Trumbull
New London, Connecticut 06320
Attn: Technical Library

U. S. Naval Weapons Laboratory
Dahlgren, Virginia 22448
Attn: Technical Library

The Franklin Institute
Benjamin Franklin Parkway at 20th Street
Philadelphia, Pennsylvania 19103
Attn: Library

Power Information Center
University City Science Institute
3401 Market Street, Room 2107
Philadelphia, Pennsylvania 19104

Aerojet-General Corporation
Von Karman Center
Azusa, California 91702
Attn: Library

Aerojet-General Nucleonics
San Ramon, California 94583
Attn: Library

University of Arizona
Department of Aerospace and
Mechanical Engineering
Tucson, Arizona 85721
Attn: Professor Kececioğlu

AiResearch Manufacturing Company
9851 Sepulveda Boulevard
Los Angeles, California 90045
Attn: Library

AiResearch Manufacturing Company
402 South 36th Street
Phoenix, Arizona 85034
Attn: Library

General Electric Company
Flight Propulsion Division
Cincinnati, Ohio 45215
Attn: Library

General Electric Company
Mechanical Technology Laboratory
Research and Development Center
Schenectady, New York 12301
Attn: Library

DOCUMENT CONTROL DATA - R & D

(Security classification of title, body of abstract and indexing annotation must be entered when the overall report is classified)

1. ORIGINATING ACTIVITY (Corporate author) University of Tennessee Mechanical & Aerospace Engineering Dept. Knoxville, Tennessee 37916		2a. REPORT SECURITY CLASSIFICATION Unclassified	
		2b. GROUP --	
3. REPORT TITLE An Investigation of Interface Stability and its Relation to Gas Ingestion in Viscoseals.			
4. DESCRIPTIVE NOTES (Type of report and inclusive dates) Interim - August 1969			
5. AUTHOR(S) (First name, middle initial, last name) Charles F. Fisher, Jr.			
6. REPORT DATE February 1969	7a. TOTAL NO. OF PAGES 69	7b. NO. OF REFS 17	
8a. CONTRACT OR GRANT NO. NGR-43-001-003 and N00014-68-A-0144	9a. ORIGINATOR'S REPORT NUMBER(S) ME 69-T57-6		
b. PROJECT NO.	9b. OTHER REPORT NO(S) (Any other numbers that may be assigned this report) --		
c.			
d.			
10. DISTRIBUTION STATEMENT This document has been approved for public release and sale; its distribution is unlimited.			
11. SUPPLEMENTARY NOTES None		12. SPONSORING MILITARY ACTIVITY --	
13. ABSTRACT A fundamental study of the stability of a dynamic gas-liquid interface between rotating cylinders is reported. The study was initiated for the purpose of seeking factors which have a significant role in the process of gas ingestion, or gas entrainment, in viscoseals. The simplified model of smooth, cylindrical surfaces was selected for mathematical tractability and to provide a visual study, using a transparent acrylic housing, without the obscurity of the more complex fluid flow resulting from the presence of the grooved surfaces employed in viscoseals. The visual study was supplemented by employing stroboscopic photography and high-speed motion picture photography. A phenomenological mechanism of gas ingestion was established, theoretically and experimentally. It was found that gas entrainment can result from a gas-liquid interface instability caused by a velocity of a portion of the interface toward the more viscous fluid and/or an acceleration of a portion of the interface toward the more dense fluid. Results of the study indicate that surface tension tends to stabilize the interface and prevent or delay gas ingestion. It is concluded that gas ingestion in viscoseals is an essentially inherent phenomenon which cannot be readily eliminated through optimization of the viscoseal geometry. A brief discussion is given on the implications of the interface stability study in the operation of journal bearings, face seals, and buffered bushing seals, in addition to a discussion of its application to viscoseals.			

14.	KEY WORDS	LINK A		LINK B		LINK C	
		ROLE	WT	ROLE	WT	ROLE	WT
	Interface Stability, Viscoseal, Sealing, Gas Ingestion, Surface Tension						